

1 Spatial and temporal dynamics of suspended sediment concentrations in coastal waters of South  
2 China Sea, off Sarawak, Borneo: Ocean colour remote sensing observations and analysis

3 Jenny Choo<sup>1</sup>, Nagur Cherukuru<sup>2</sup>, Eric Lehmann<sup>2</sup>, Matt Paget<sup>2</sup>, Aazani Mujahid<sup>3</sup>, Patrick Martin<sup>4</sup>, Moritz Müller<sup>1</sup>

4 <sup>1</sup>Swinburne University of Technology, Faculty of Engineering, Computing and Science, Jalan Simpang Tiga, 93350 Kuching,  
5 Sarawak, Malaysia.

6 <sup>2</sup>Commonwealth Scientific and Industrial Research Organization (CSIRO), Canberra ACT 2601, Australia.

7 <sup>3</sup>Faculty of Resource Science & Technology, University Malaysia Sarawak, Kota Samarahan 94300, Sarawak, Malaysia.

8 <sup>4</sup>Asian School of the Environment, Nanyang Technological University, 639798, Singapore.

9

10 Correspondence to: Jenny Choo (JChoo@swinburne.edu.my/jccy89@gmail.com)

11

12 Abstract

13 High-quality ocean colour observations are increasingly accessible to support various monitoring and  
14 research activities for water quality measurements. In this paper, we present a newly developed  
15 regional total suspended solids (TSS) empirical model using MODIS-Aqua's Rrs(530) and Rrs(666)  
16 reflectance bands to investigate the spatial and temporal variation of TSS dynamics along the  
17 southwest coast of Sarawak, Borneo. The performance of this TSS retrieval model was evaluated using  
18 error metrics (bias = 1.0, MAE = 1.47, and RMSE = 0.22 in mg/L) with a log<sub>10</sub> transformation prior to  
19 calculation, as well as a k-fold cross validation technique. The temporally averaged map of TSS  
20 distribution, using daily MODIS-Aqua satellite datasets from 2003 until 2019, revealed large TSS  
21 plumes detected particularly in the Lupar and Rajang coastal areas on a yearly basis. The average TSS  
22 concentration ~~in these coastal waters was in the~~ range of 15 – 20 mg/L. ~~was estimated at these coastal~~  
23 ~~areas.~~ Moreover, the spatial map of TSS coefficient of variation (CV) indicated strong TSS variability  
24 (approximately 90 %) in the Samunsam-Sematan coastal areas, which could potentially impact nearby  
25 coral reef habitats in this region. ~~Our findings-~~ Study on temporal TSS variation provide further  
26 evidence that monsoonal patterns drive the TSS release in these tropical water systems, with distinct  
27 and widespread TSS plume variations observed between the northeast and southwest monsoon  
28 periods. ~~A m~~Map of relative TSS distribution anomalies revealed strong spatial TSS variations in the  
29 Samunsam-Sematan coastal areas, while 2010 recorded a major increase (approximately 100 %) and  
30 widespread TSS distribution with respect to the long-term mean. Furthermore, ~~study your findings~~ on  
31 the contribution of river discharge to the TSS distribution showed a weak correlation across time at  
32 both the Lupar and Rajang river mouth points. The variability of TSS distribution across coastal river  
33 points was studied by investigating the variation of TSS pixels at three transect points, stretching from  
34 the river mouth into territorial and open water zones, for eight main rivers. ~~Results~~Our findings  
35 showed a progressively decreasing pattern of nearly 50 % in relation to the distance from shore, with  
36 exceptions in the northeast regions of the study area. Essentially, our findings demonstrate that the  
37 TSS levels at the southwest coast of Sarawak are within local water quality standards, promoting  
38 various marine and socio-economic activities. This study presents the first observation of TSS  
39 distributions at Sarawak coastal systems with the application of remote sensing technologies, to  
40 enhance coastal sediment management strategies for the sustainable use of coastal waters and their  
41 resources.

42 Keywords: total suspended solids, band-ratio, monsoon, river discharge, Open Data Cube

43

44

45

46 1.0 Introduction

47 Total Suspended Solids (TSS) play an important role in the aquatic ecosystem as one of the primary  
48 water quality indicators of coastal and riverine systems (Alcántara et al., 2016; Cao et al., 2018; Chen  
49 et al., 2015a; González Vilas et al., 2011; Mao et al., 2012). For example, elevated concentrations of  
50 TSS in water have an adverse impact on fisheries and biodiversity of the aquatic ecosystem (Bilotta  
51 and Brazier, 2008; Chapman et al., 2017; Henley et al., 2000; Wilber and Clarke, 2001). Understanding  
52 the impacts of varying water quality in relation to TSS status has been one of the primary concerns  
53 with respect to a country's growing Blue Economy status and sustainable management of aquatic  
54 resources (Lee et al., 2020a; Sandifer et al., 2021; World Bank and United Nations Department of  
55 Economic and Social Affairs (UNDESA), 2017). With about 40 % of the world's population living within  
56 100 km of coastal areas (United Nations, 2017), and with more than 80 % of the population in Malaysia  
57 living within 50 km of the coast (Praveena et al., 2012), water quality monitoring and management  
58 efforts are important at both regional and global scale.

59 Studying TSS distribution can provide insights into the connections between land and ocean  
60 ecosystems (Howarth, 2008; Lemley et al., 2019; Lu et al., 2018). For instance, TSS dynamics allow us  
61 to understand the impacts of sediment transport and sediment plumes, particularly in areas  
62 experiencing large-scale deforestation, land conversion and damming of rivers (Chen et al., 2007;  
63 Espinoza Villar et al., 2013). Sarawak, Malaysian Borneo, experienced significant land use and land  
64 cover change activities over the past four decades, with widespread land conversion and deforestation  
65 for developments and large-scale plantation activities (Gaveau et al., 2016), as well as building of  
66 major road infrastructures, such as the Pan-Borneo highway, and hydroelectric dams (Alamgir et al.,  
67 2020). As a result, river and coastal systems may potentially drive large TSS loads into downstream  
68 systems and into the marine and open ocean waters.

69 Situated at the southern part of the South China Sea, the region of Sarawak, Malaysian  
70 Borneo, has a coastline of about 1035 km where mangrove forests are dominant (Long, 2014). The

71 coastal regions of Sarawak are rich with marine coastal biodiversity and coral reefs, which can be  
72 found at the northeast and southwest part of Sarawak (Praveena et al., 2012). While the coasts of  
73 Sarawak provide important socio-economic values to the local communities (Lee et al., 2020b), these  
74 coastal areas are potentially facing water quality degradation from TSS riverine outputs in response  
75 to land use and land cover change activities.

76 TSS concentrations are commonly measured through conventional laboratory-based methods  
77 to quantify TSS concentrations by field collection of water samples (Ling et al., 2016; Mohammad Razi  
78 et al., 2021; Soo et al., 2017; Soum et al., 2021; Tromboni et al., 2021; Zhang et al., 2013). Currently,  
79 real-time high-frequency TSS observations using modern optical and bio-sensor systems are also  
80 possible (Bhardwaj et al., 2015; Horsburgh et al., 2010). These sensors can be generally found onboard  
81 ship and buoy-based observation platforms. Yet, it remains a challenge to quantify TSS concentrations  
82 of large spatial coverage and high temporal frequency with these approaches.

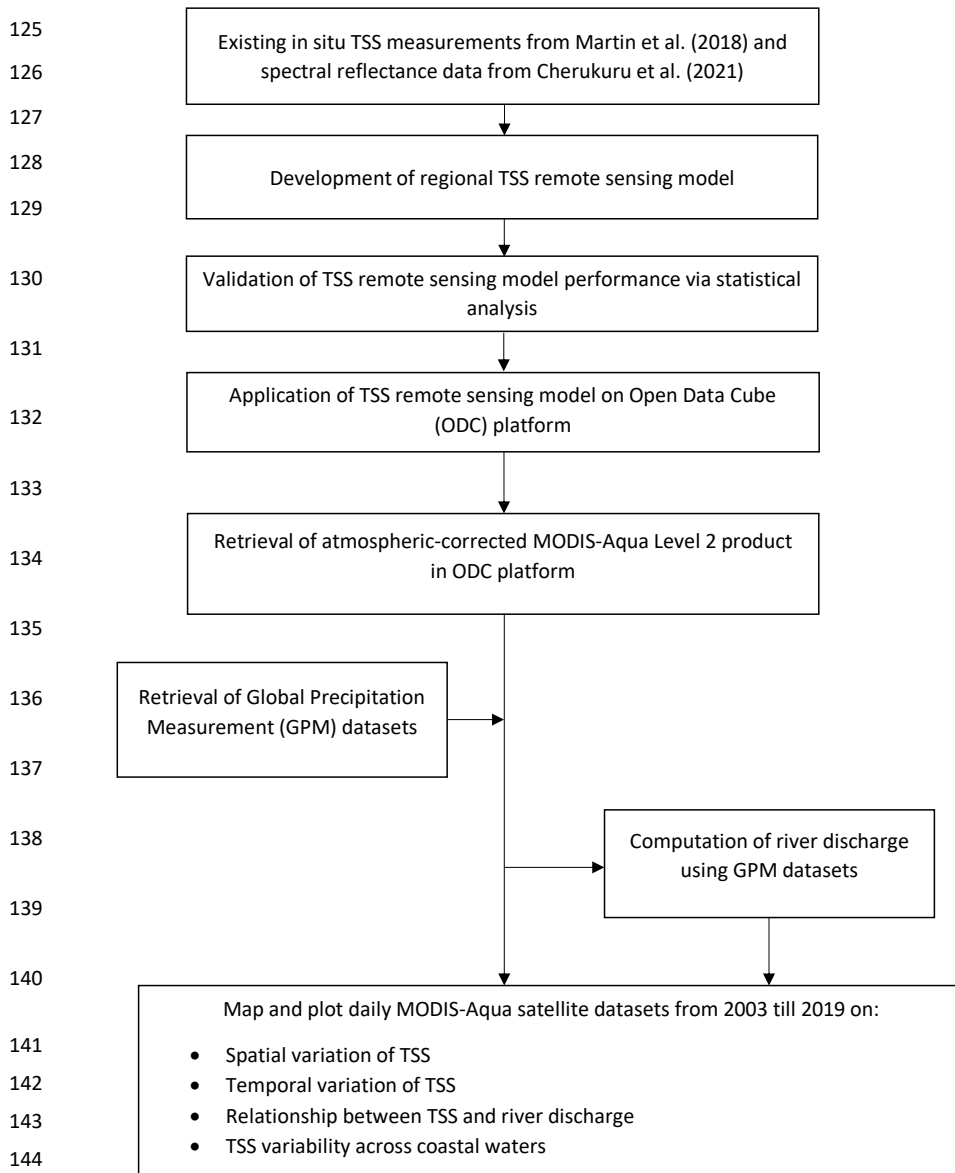
83 Ocean colour remote sensing technologies represent an increasingly accessible and powerful  
84 tool to provide a synoptic view for short or long-term water quality studies at high temporal and spatial  
85 resolutions (Cherukuru et al., 2016a; Slonecker et al., 2016; Swain and Sahoo, 2017; Wang et al., 2017;  
86 Werdell et al., 2018). Remote sensing can help overcome several constraints of conventional intensive  
87 field campaigns such as: (i) costly field campaigns from boat rentals or cruise; (ii) time-consuming and  
88 inadequate manpower; and most importantly for this study, (iii) limited spatial and temporal field  
89 coverage. NASA's Moderate Resolution Imaging Spectroradiometer (MODIS)-Aqua  
90 (<https://modis.gsfc.nasa.gov/about/>) has a distinctive advantage with its daily revisit time, a spatial  
91 resolution of 250 – 1000 m, and a large collection of ocean colour data since 2002. Other sensors  
92 offering ocean colour measurement capabilities include Landsat-8, which, in comparison with MODIS-  
93 Aqua, has a 16-day revisit time and high spatial resolution of 30 m. Despite Landsat's powerful ability  
94 in capturing higher resolution images, the longer revisit interval may not be suitable for characterizing  
95 and studying water bodies with high dynamics of various water constituents.

96 Several MODIS-derived models have been developed for TSS retrievals (Chen et al., 2015b;  
97 Espinoza Villar et al., 2013; Jiang and Liu, 2011; Kim et al., 2017; Zhang et al., 2010b), including  
98 empirical, semi-analytical and machine-learning approaches (Balasubramanian et al., 2020; Jiang et  
99 al., 2021). However, the performance of these models proved to be less satisfactory, with recorded  
100 low  $r^2$  and high bias and mean absolute error (MAE) values when tested with in situ TSS datasets  
101 (Supplementary Materials, Table S1). While these global TSS remote sensing models address the need  
102 to improve TSS retrievals and to monitor global TSS trends in various water class types, they tend to  
103 underperform in more localised and regional studies (Mao et al., 2012; Ondrusek et al., 2012). The  
104 coastal waters of Borneo are well-mixed throughout the year and enriched with suspended material  
105 and dissolved organic matter (Müller et al., 2016). Various water quality studies of the river systems  
106 have been actively carried out to assess the dynamics of numerous water quality constituents in  
107 response to human activities, with TSS concentrations being one of the primary environmental  
108 concerns in this region (Ling et al., 2016; Müller-dum et al., 2019; Tawan et al., 2020). Although studies  
109 on the water quality of coastal systems in Borneo have gradually gained much attention (Cherukuru  
110 et al., 2021; Limch et al., 2010; Martin et al., 2018; Soo et al., 2017), there is still much knowledge to  
111 gain on the understanding of how coastal waters in the region have been impacted by TSS loadings  
112 and transport over large spatial and temporal scales.

113 Here, in this paper, we present a new regional empirical TSS remote sensing model. While  
114 various remote sensing models have their own unique computational strengths, this ~~studypaper~~  
115 demonstrates the reliability of band ratio TSS model to be applied within optically complex waters.  
116 With the ongoing efforts to address and minimize water quality degradation in coastal systems, as  
117 outlined in the United Nation's Sustainability Development Goals no. 14, our study aims to apply the  
118 new empirical regional TSS remote sensing model to: (a) investigate the spatial and temporal  
119 variability in TSS, (b) identify hotspots of TSS distribution in the coastal waters of Sarawak, Malaysian  
120 Borneo, using a long time series of MODIS-Aqua data from year 2003 until 2019, and (c) study the  
121 varying monsoonal and river discharge patterns in relation to TSS distribution at river mouths.

122 2.0 Methodologies

123 Figure below summarizes the processes carried out in this study. Spatial and temporal variation of TSS  
124 distribution was mapped using atmospheric-corrected MODIS-Aqua Level 2 product.



145 Fig. 1: Flowchart summarizing the processes of developing a regional TSS remote sensing model and applying it to analyse  
146 the spatial and temporal variation of TSS over the study region, using MODIS-Aqua data from year 2003 until 2019. Long-  
147 term MODIS-Aqua datasets were analysed and mapped on an Open Data Cube (ODC) platform with implementation of robust  
148 Python libraries and packages.

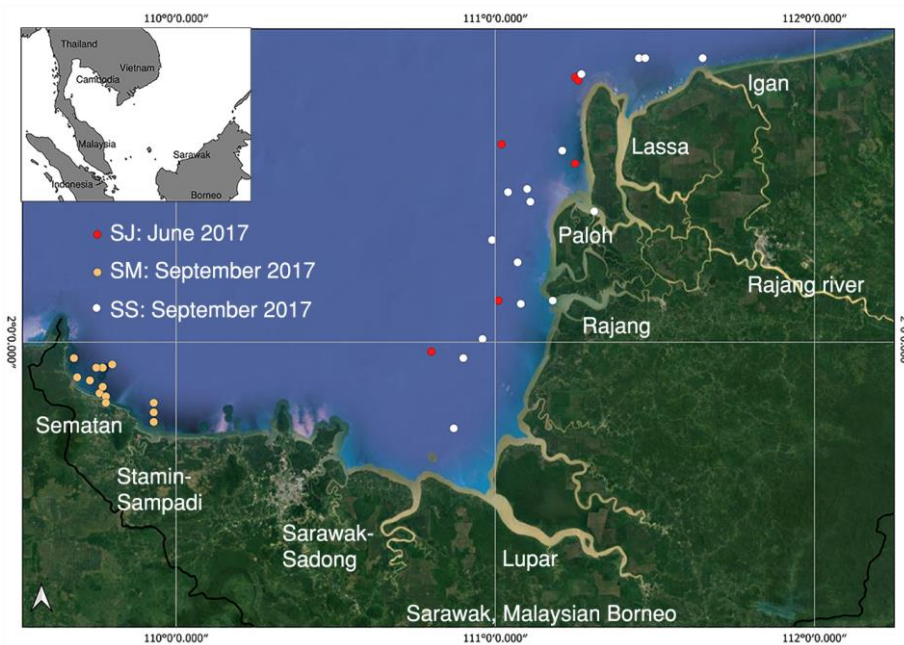
149

## 150 2.1 Area of study

151 Our study focuses on the southwestern coast of Sarawak (between 1.9° N, 109.65° E and 2.8° N, 111.5°  
152 E) in Malaysia, which sits at the northwest part of the Borneo Island. Generally, the island of Borneo  
153 (between 3.01° S, 112.18° E and 6.45° N, 117.04° E) contains rich tropical rainforests and biodiversity  
154 on the lands of Sarawak and Sabah (Malaysia), Brunei, and Indonesia. Typically, Sarawak is a tropical  
155 climate region, recording an average ambient temperature of 27.8 °C (variation of 1.8 °C) throughout  
156 the year. It records high precipitation with an average of 4116.7 mm/yr in Kuching (1.5535° N,  
157 110.3593° E), the capital city of Sarawak. Yearly, it experiences both a dry and wet season, which is  
158 influenced by: (i) the southwestern monsoon (May to September) and (ii) the northeastern monsoon  
159 (November to March). Rivers in Sarawak are connected to the South China Sea and flow through  
160 various plantation types, such as oil palm, rubber and sago (Davies et al., 2010).

161 In this study, the southwestern part of Sarawak's coastal regions (Fig. 2), (between 1.9° N, 109.65° E  
162 and 2.8° N, 111.5° E) was studied, which comprise several major rivers (e.g. Lupar, Sebuyau, Sematan),  
163 as well as the Rajang River, the longest river in Malaysia. Rajang river basin consists in tidally influenced  
164 river channel which splits into a northwest (Igan, Lassa and Paloh) and a southwest (Rajang, Belawai)  
165 Rajang river delta (Staub et al., 2000). The Rajang river basin drains a dominant area (>50,000km<sup>2</sup>) of  
166 sedimentary rocks (Milliman and Farnsworth, 2013; Staub et al., 2000) extending from Belaga to Sibu,  
167 with major peatland areas converted into oil palm plantations (Gaveau et al., 2016) as its river flows  
168 into the South China Sea (Milliman and Farnsworth, 2013). Major settlements along the Rajang river  
169 comprise of Kapit and Kanowit town areas, as well as Sibu city, with a total population size of about  
170 388,000 inhabitants (Department of Statistics, 2020). Lupar and Saribas rivers, respectively, comprise  
171 a catchment area size of approximately 6500 and 1900 km<sup>2</sup> (Lehner et al., 2006). Situated at the  
172 southwest side of the Rajang catchment, Lupar and Saribas rivers surround the Maludam National

173 [Park, which is Sarawak's remaining biggest single patch of peat swamp forest \(Sarawak Forestry](#)  
174 [Corporation, 2022\)](#). Adjacent to Lupar river mouth is the Sadong river, with an approximate catchment  
175 [area size of 3500 km<sup>2</sup> \(Kuok et al., 2018\)](#). Sadong river runs about 150 km and flows through oil palm  
176 [plantations \(Staub and Esterle, 1993\)](#). These river systems are associated with increasing land use  
177 activities and land cover changes in this region, which essentially transport and connect various  
178 biogeochemical water components to the coastal systems of Sarawak.



179 Fig. 2: Map of the study area (© Google Maps), located in the southwestern part of Sarawak, Malaysia (inset). Indicators  
180 show the location of sampling sites used during field expeditions carried out in June and September 2017.  
181

## 182 2.2 In situ TSS measurements

183 TSS measurements ~~data~~ were taken from Martin et al. (2018). A total of 35 coastal sites were studied  
184 and are denoted SJ, SS, and SM (see: Table 1 & Fig. 2). These water samples were collected in the  
185 month of June (SJ region) and September (SS and SM regions) in 2017. Water samples were filtered,

186 and filters were dried and ashed prior to weighing process. Full details of water sampling and TSS  
187 analysis is available in Martin et al. (2018).

### 188 2.3 Development, calibration and validation of TSS model

189 In situ remote sensing reflectance spectral data,  $R_{rs}(\lambda)$ , along with 35 measured TSS values, were used  
190 to develop a new remote sensing TSS empirical model for MODIS-Aqua for this case study. Field  
191 measurements of SM, SJ & SS datasets, as shown in Table 1, were used to calibrate the MODIS-Aqua  
192 TSS remote sensing model.

193 For the in situ remote sensing reflectance,  $R_{rs}(\lambda)$  readings, a TriOS-RAMSES spectral imaging  
194 radiometer was used to measure downwelling irradiance,  $E_d(\lambda)$ , and upwelling radiance,  $L_u(\lambda)$ , with  
195 measurement protocols from Mueller et al. (2002). These measurements were recorded under stable  
196 sky and sea conditions during the day (10AM to 4PM) with [high solar elevation angles. high-sun](#)  
197 ~~elevation-angle-condition.~~

198 Measurements of reflectance,  $R_{rs}(\lambda)$ , were recorded concurrently with the collection of water samples  
199 (as described in Section 2.2) and were recorded at wavelength ranging from 280 to 950 nm, which  
200 covers the spectrum of ultraviolet, visible and visible/ultraviolet light. These measurements were  
201 recorded on a float to capture  $L_u(0-, \lambda)$  and  $E_d(0+, \lambda)$ , where 0- and 0+ refer to below-surface and  
202 above-surface, respectively.

203 Remote sensing reflectance,  $R_{rs}(\lambda)$ , was computed as follows with reference to Mueller et al. (2002):

$$R_{rs}(\lambda, 0+) = \frac{1 - p}{n^2} \times \frac{L_u(0-, \lambda)}{E_d(0+, \lambda)} \quad (1)$$

204 where  $p = 0.021$  refers to the Fresnel reflectance and  $n = 1.34$  is the refractive index of water. Full  
205 details of this methodology can be found at Cherukuru et al. (2021).

#### 206 2.3.1 Calibration of empirical model and application to MODIS-Aqua



207 With the intention to apply a regional TSS remote sensing model to MODIS-Aqua product, a total  
208 number of 35 different TSS datasets of TSS concentrations were collected in coastal conditions (salinity  
209 > 15 PSU) and convolved to generate MODIS-Aqua data.

210 In this study, retrieval of water constituents was established using spectral band ratio combinations  
211 which have proven to be a straightforward, yet reliable method for estimating water constituents in  
212 optically turbid waters (Ahn and Shanmugam, 2007; Cao et al., 2018; Lavigne et al., 2021; Morel and  
213 Gentili, 2009; Neil et al., 2019; Siswanto et al., 2011). Band ratio models help to offset signal noise,  
214 such as the effects of atmospheric and irradiance of spectral reflectance to a certain degree  
215 (Cherukuru et al., 2016b; Ha et al., 2017; Hu et al., 2012; Liu et al., 2019).

216 A variety of models using single bands, as well as a combination of MODIS-Aqua's Blue, Green & Red  
217 bands (412nm, 440nm, 488nm, 532nm, 555nm & 660nm) were calibrated using field measurements  
218 as dependent variable. The calibration process was tested out using various model functions, including  
219 linear, power, exponential, and logarithm functions. The best empirical TSS retrieval model was fitted  
220 by means of a regression between the in situ TSS data and in situ radiometer values, and can be  
221 expressed as follows:

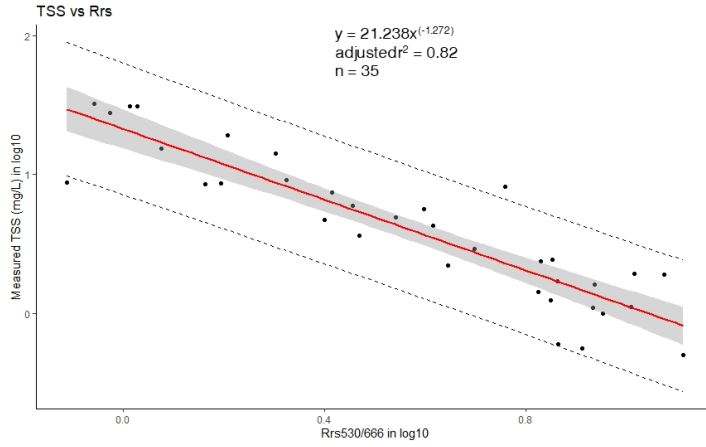
$$222 \quad \text{TSS} = 21.238[\text{Rrs}(530)/\text{Rrs}(666)]^{-1.272} \quad (2)$$

223 This power function model resulted in a coefficient of determination ( $R^2$ ) of 0.82 (Fig. 3).

224 Table 1: Summary statistics of TSS values collected at areas SJ, SS, and SM located within coastal regions in this study, with a  
225 total of 35 datasets recorded.

Coastal Area	Minimum	Maximum	Mean	S.D.	C.V.	n
SJ	1.1	19.24	6.89	6.62	96.09	6
SS	0.56	32.1	12.50	11.43	91.45	16
SM	0.5	8.14	2.59	2.70	104.53	13

226



227  
 228 Fig. 3: Empirical relationship of TSS retrieval between in situ Rrs(530)/Rrs(666) bands ratio and measured TSS  
 229 concentration (mg/L), as established via a power law function. Upper and lower dashed lines indicate the 95 % prediction  
 230 interval of the regression.

231 2.3.2 Performance assessment and validation of MODIS-Aqua empirical model

232 ~~An evaluation of the model was performed using a k-fold cross-validation technique (Refaeilzadeh et~~  
 233 ~~al., 2020) given the small size of the TSS dataset used in this study (Table 2). A selection of k = 7 was~~  
 234 ~~assigned to split the datasets into k groups with an equal number of data points.~~

235 An assessment of the performance error of the newly developed TSS model was carried out as per  
 236 Seegers et al. (2018)'s recommendation for interpreting ocean colour models. These performance  
 237 metrics used here include the bias, Mean Absolute Error (MAE), Root Mean Squared Error (RMSE),  
 238 coefficient of variation (CV), as well as the coefficient determination,  $r^2$ , based on the following  
 239 calculations:

240 
$$\text{Bias} = 10^{\wedge} \left[ \frac{\sum_{i=1}^n \log_{10}(M_i) - \log_{10}(O_i)}{n} \right] \quad (3)$$

241 
$$\text{MAE} = 10^{\wedge} \left[ \frac{\sum_{i=0}^n | \log_{10}(M_i) - \log_{10}(O_i) |}{n} \right] \quad (4)$$

242 
$$\text{RMSE} = \sqrt{\frac{\sum_{i=1}^n (\log_{10}(M_i) - \log_{10}(O_i))^2}{n}} \quad (5)$$

243 
$$\text{CV} = \frac{\sigma}{\mu} \times 100\% \quad (6)$$

244 where M represents the modelled TSS values, n is the number of samples, and O represents the  
 245 observed TSS measurements, while  $\sigma$  refers to standard deviation and  $\mu$  represents the mean value.  
 246 Equations (3), (4) and (5) use a log<sub>10</sub>-transform of the data as the range of TSS values can span several  
 247 orders of magnitude. As such, an application of the log-transform prior to error metric calculation  
 248 allows us to account for uncertainties that are proportional to the concentration values  
 249 (Balasubramanian et al., 2020; Seegers et al., 2018).

250 **Table 2: Calibration and accuracy assessment of the newly derived MODIS-Aqua models in this study for TSS estimations**  
 251 **tested using various model functions. Calculation for bias, MAE and RMSE use a log-transform of the data prior to calculation**  
 252 **of error metric measurements, as adapted from Seegers et al. (2018) and Balasubramanian et al. (2020). Band ratio**  
 253 **Rrs(530)/Rrs(666) is established as function x. Power function model is selected based on low performance metric values.**

Formatted: Justified

Model	Function	Bias	MAE	RMSE	CV (%)	R
Power	$TSS = 21.238x^{-1.272}$	0.9999	1.4732	0.2161	4.74	0.84
Linear	$TSS = -1.8193x + 16.928$	1.4463	1.8549	6.7174	20.699	0.6854
Exponential	$TSS = 17.784e^{-0.296x}$	1.0791	1.4906	6.3088	3.8920	0.8154
Logarithmic	$-8.872\ln(x)+19.383$	1.1336	1.6177	5.3735	-17.056	0.8128

254

255 **Table 2: Assessment of fitting error for the proposed TSS model, using k-fold cross validation.**

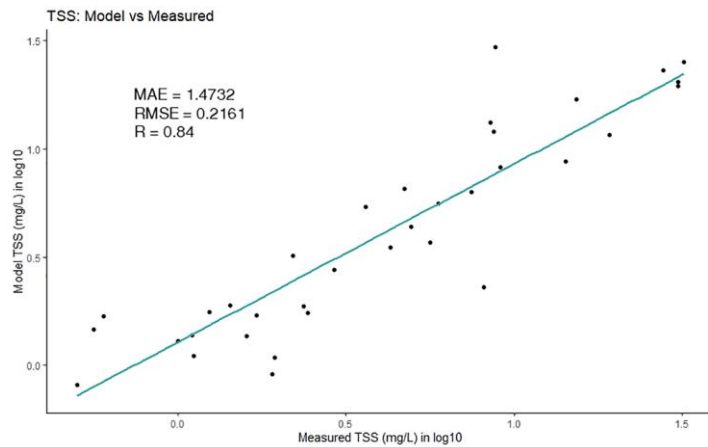
Parameter	k-fold (n)	R2	RMSE	MAE
TSS	7	0.85	0.2159	0.1747

256

257 **Table 3: Calibration and accuracy assessment of the newly derived MODIS-Aqua models in this study for TSS estimations.**  
 258 **Calculation for bias, MAE and RMSE use a log-transform of the data prior to calculation of error metric measurements, as**  
 259 **adapted from Seegers et al. (2018) and Balasubramanian et al. (2020).**

Parameter	Bands (nm)	Model	Bias	MAE	RMSE	CV (%)	R
TSS	Rrs(530), Rrs(666)	$TSS = 21.238 \left( \frac{Rrs(530)}{Rrs(666)} \right)^{-1.272}$	0.9999	1.4732	0.2161	4.74	0.84

260



261

262 Fig. 4: Scatterplot of modelled TSS values derived from the proposed model and measured TSS values (mg/L). ~~Check~~  
263 ~~decimals in figure~~

264 An evaluation of the model was performed using a k-fold cross validation technique (Refaeilzadeh et  
265 al., 2020) given the small size of the TSS dataset used in this study (Table 2). A selection of k = 7 was  
266 assigned to split the datasets into k groups with an equal number of data points.

267 Table 2: Assessment of fitting error for the proposed TSS model, using k-fold cross validation.

<u>Parameter</u>	<u>k-fold (n)</u>	<u>R2</u>	<u>RMSE</u>	<u>MAE</u>
<u>TSS</u>	<u>7</u>	<u>0.85</u>	<u>0.2159</u>	<u>0.1747</u>

268

269 While these results point to low error levels achieved by the proposed regional TSS retrieval model  
270 (Table 3, Fig. 4), caution should be used when applying it to various water types. Water type  
271 classification has been thoroughly described by Balasubramanian et al. (2020) where waters are  
272 classed into Type I (Blue-Green waters), Type II (Green waters), and Type III (Brown waters).  
273 Essentially, the Green-to-Red band ratio is optimised with these datasets corresponding to sediment-  
274 dominated and yellow-substance loaded water conditions. As highlighted by Morel & Belanger (2006),  
275 ~~waters of this type do not have the same spectral characteristics as phytoplankton-rich waters this~~  
276 ~~type of waters is not spectrally consistent to phytoplankton-rich waters~~ (also known as Case 1 waters).  
277 In addition to the impact on water clarity, sediment particles (often red-brownish coloured) also tend

278 to enhance the backscattering and absorption properties, especially at shorter wavelengths (Babin et  
279 al., 2003), while the additional presence of coloured dissolved matter (yellow substance) leads to  
280 strong absorption properties at short wavelengths. As the TSS retrieval model was developed from  
281 samples taken in waters that are bio-optically rich in suspended solids and dissolved organic matter,  
282 an application of this TSS model needs to be done cautiously when applying to other water types,  
283 particularly those with large concentration of phytoplankton.

#### 284 2.4 Application of TSS retrieval model

285 Daily MODIS-Aqua satellite data from year 2003 to 2019 (total of 6192 individual time slices) were  
286 studied with a 2°x 2° spatial resolution (longitude: 109.38, 112.0; latitude: 1.22, 3.35) which covers  
287 the southwestern coastal region of Sarawak and southern part of the South China Sea.  
288 Atmospherically corrected MODIS-Aqua level 2 reflectance products (Bailey et al., 2010; NASA Official,  
289 n.d.) were retrieved for the application of the TSS model proposed in this study. Negative remote  
290 sensing reflectance values, possibly due to failure of atmospheric correction, were filtered out before  
291 applying the retrieval model, as expressed in Eq. (2), to map the spatial and temporal distribution of  
292 TSS estimates. In addition, averaging of spatial and temporal TSS variation maps in this study was  
293 carried out by filtering TSS values with fewer than 10 valid data points over the whole time series,  
294 along with application of sigma clipping operation ([refer to:  
295 https://docs.astropy.org/en/stable/api/astropy.stats.sigma\\_clip.html](https://docs.astropy.org/en/stable/api/astropy.stats.sigma_clip.html)).

##### 296 2.4.1 Open Data Cube

297 In this study, the analysis of remote sensing data over large spatial extents and at high temporal  
298 resolution was carried out using robust Python libraries and packages run on an Open Data Cube (ODC)  
299 platform. Open Data Cube is an open-source advancement in computing technologies and data  
300 architectures which addresses the growing volume of freely available Earth Observation (EO) satellite  
301 products (Giuliani et al., 2020; Killough, 2019). ODC provides a collection of software which index,  
302 manage, and process large EO datasets such as satellite products from the MODIS, Landsat and

303 Sentinel missions (Gomes et al., 2021). These satellite datasets are structured in a multi-dimensional  
304 array format, and provide layers of information across latitude and longitude (Open Data Cube, 2021).  
305 Leveraging the growing availability of Analysis Ready Data (ARD), and with support from the  
306 Committee of Earth Observation Satellites (CEOS) (Killough, 2019), the ODC concept has been  
307 deployed in many countries across the world. These existing deployments include Digital Earth Africa  
308 (<https://www.digitalearthafrika.org/>), Digital Earth Australia (DEA) (<https://www.dea.ga.gov.au/>),  
309 Vietnam Open Data Cube (<http://datacube.vn/>), and Brazil Data Cube ([https://github.com/brazil-data-](https://github.com/brazil-data-cube)  
310 [cube](https://github.com/brazil-data-cube)), which provide various time-series datasets of the changing landscape and water content in  
311 these specific regions (Giuliani et al., 2020; Gomes et al., 2021; Killough, 2019; Lewis et al., 2017). The  
312 ecosystem and architecture of ODC is well explained at [opendatacube.org](https://opendatacube.org). The codes and tools used  
313 in this application drew upon the information provided in various DEA notebooks (Krause et al. (2021),  
314 which can be found at <https://github.com/GeoscienceAustralia/dea-notebooks/>.

### 315 2.5 Precipitation data and computation of river discharge

316 Monthly precipitation values (mm) over the Lupar and Rajang basins were extracted from the Global  
317 Precipitation Measurement (GPM) Level 3 IMERG satellite datasets  
318 (<https://gpm.nasa.gov/data/imerg>) (Supplementary Materials, Fig. S4 – 7) in order to assess the  
319 influence of precipitation in each river basin in relation to TSS concentration at the corresponding river  
320 mouth (Supplementary Materails, Fig. S4 – 7).

321 Derivation of river discharge ( $\text{m}^3/\text{s}$ ) was computed using total precipitation estimates (mm) over each  
322 river basin, and multiplied by a surface discharge runoff factor for the studied region (Sim et al., 2020).  
323 The surface runoff was estimated to be 60 % of total precipitation (Staub et al., 2000; Whitmore,  
324 1984). ~~Precipitation data were extracted from the monthly NASA Global Precipitation Measurement~~  
325 ~~(GPM) Level 3 IMERG dataset (<https://gpm.nasa.gov/data/imerg>).~~ In this study, the Rajang river basin,  
326 as well as the combined basins of the Lupar, Sadong, and Saribas rivers (hereafter referred to as the  
327 Lupar basin), were studied for their river discharge rates in relation to TSS release.

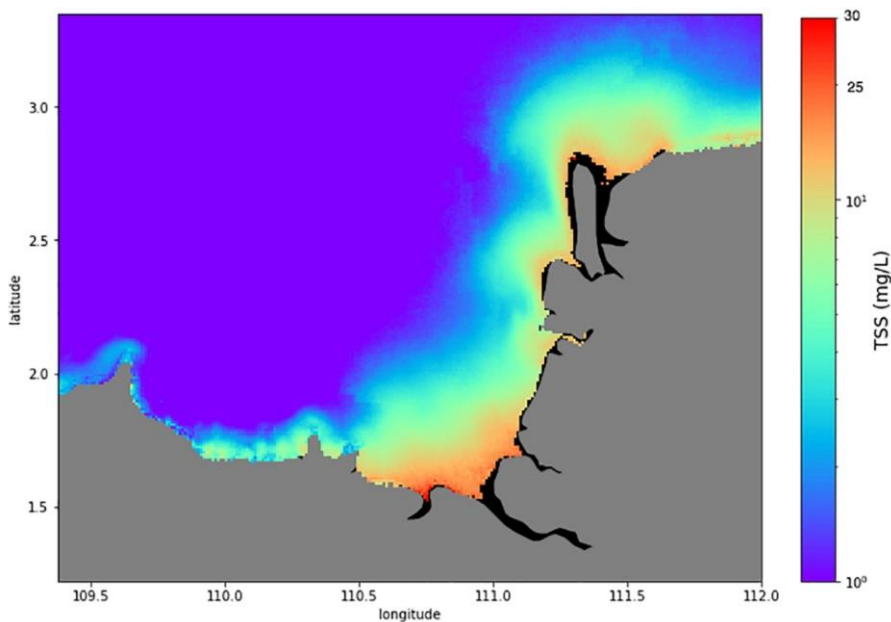
## 328 3.0 Results & Discussion

### 329 3.1 Spatial variation of TSS distribution

330 Changes in TSS distribution occur across space and time. The regional TSS remote sensing model  
331 calibrated in this study was applied to the time series of MODIS-Aqua data to study the variability of  
332 spatial TSS distribution and identify potential hotspot areas susceptible to TSS water quality  
333 degradation. The map of average TSS for the Sarawak region was generated (Eq. 2) by averaging all  
334 the daily MODIS-Aqua TSS images (2003 to 2019) and is presented in Fig. 5. The results show that the  
335 waters in the northeast region of the study area, stretching from the Sadong river to the Rajang/Igan  
336 river have seen sustained levels of TSS over the 17 years considered in this study.

337 The temporally averaged spatial distribution map (Fig. 5) shows TSS concentrations in the range of 15  
338 – 20 mg/L near the river mouth areas, with widespread TSS plumes extending into the South China  
339 Sea (Fig. 5). Based on the Malaysia Marine Water Quality Criteria and Standard (Supplementary  
340 Materials, Table S2) (Department of Environment, 2019), these coastal waters fall under Class 1 in  
341 relation to their TSS (mg/L) status. This classification indicates that these coastal waters support and  
342 preserve marine life in this local region. Yet, several studies have expressed concerns regarding high  
343 TSS loadings in riverine waters owing to the impacts of various land use and land cover changes (LULC)  
344 (Ling et al., 2016; Tawan et al., 2020). Among these, the Rajang river has been highlighted to be heavily  
345 impacted by various LULC activities such as large-scale deforestation and construction of hydropower  
346 dams (Alamgir et al., 2020). In situ water quality studies by Ling et al. (2016) reported on high TSS  
347 estimates at one of the upstream tributaries of Rajang river, the Baleh river, with TSS readings up to  
348 approximately 100 mg/L. Another study by Tawan et al. (2020) reported a significant TSS release  
349 reaching to 940,000 mg per day during wet seasons, with maximum TSS concentrations of 1700 mg/L  
350 in the upstream tributaries of the Rajang river, particularly at the Baleh and Pelagus rivers. The  
351 majority of the upstream tributary rivers were categorised as Class II (during dry season) and Class III  
352 (during wet season) waters according to the National Water Quality Index (Supplementary Materials,

353 Table S3) (Department of Environment, 2014), due to increased soil erosion from surrounding LULC  
354 activities (Tawan et al., 2020). These local in situ findings provide valuable insights on point source TSS  
355 estimates in these LULC change regions. Coupled with our spatial map of average TSS captured by  
356 remote sensing technologies, our findings seem to suggest that a large portion of TSS loadings from  
357 inland and upstream rivers would have settled and deposited in these river channels and were not  
358 completely discharged outwards into the coastal areas, which would have caused major water quality  
359 degradation in the corresponding coastal systems.



360  
361 Fig. 5: Temporally averaged 2°x 2° map of TSS distribution (on a log scale) across the time dimension for each pixel.

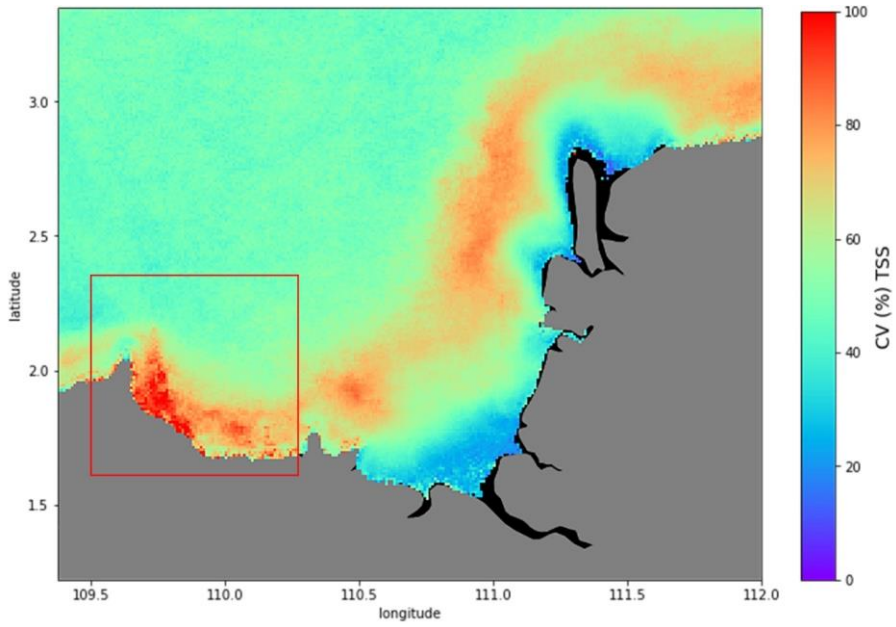
362 Historical patterns of TSS concentration were assessed by comparing annual maps of average TSS  
363 distribution (Supplementary Materials; Fig. S1), as well as time series of TSS estimates at the Lupar  
364 and Rajang river mouths (Supplementary materials; Fig. S2). From our findings, the annual TSS maps  
365 further support the observation where TSS release was evident at Lupar and Rajang/Igan river mouths  
366 from 2003 till 2019, which points to Class I of local water quality standards in relation to TSS (mg/L)



367 status. This was found to consistently occur every year. Furthermore, the TSS trend study showed that  
368 both the Lupar and Rajang river mouth points have a gradual increase of TSS concentration over the  
369 17 years (Supplementay materials; Fig. S2). This increasing trend was, however, not statistically  
370 significant ( $p = 0.43$  for Lupar, and  $p = 0.15$  for Rajang).

371 Moreover, a map of the TSS coefficient of variation (CV) was computed to identify areas with a high  
372 degree of relative TSS variation over time (Fig. 6). Here again, the map of CV (%) was produced by  
373 aggregation of the daily MODIS-Aqua images (6192 time steps) from 2003 until 2019. Figure 6 shows  
374 that the Samunsam-Sematan coastal region (as highlighted by the red box) exhibits an increased level  
375 of TSS distribution variability, with a recorded CV of more than 90 %.

376 The Samunsam-Sematan coastal region contains near-pristine mangrove forests which are sheltered  
377 from major LULC activities, as compared to other studied sites. Samunsam-Sematan is also well-known  
378 locally as a recreational hotspot with coral reefs and various national parks (Sarawak Tourism Board,  
379 2021). Data from the Centre for International Forestry Research (CIFOR) Forrest Carbon database  
380 (CIFOR, n.d.) revealed that there was more than double the amount of total forest loss (approx. 5,000  
381 Ha) recorded in Lundu, a nearby township in the Sematan area in 2011 as compared to the previous  
382 years. Deforestation activities, regardless of their scale, can inevitably promote sediment loss and soil  
383 leaching into the nearby river systems (Yang et al., 2002). Important information regarding the  
384 variability in water quality (as shown in Fig. 6) can provide support to local authorities and relevant  
385 agencies in order to identify vulnerable areas that need to be monitored closely, such as the Lundu-  
386 Sematan region in this case. The CV map thus offers interesting insights into how TSS distribution can  
387 vary across large spatial areas, which can ultimately impact local socio-economic activities in this  
388 region (Lee et al., 2020b).



389

390 Fig. 6: Map of CV (%) calculated from the daily time series of MODIS-Aqua satellite images from 2003 until 2019.

391

392

393

394

395

396

397

398

399

400

401 3.2 Temporal variation of TSS distribution

402 On a temporal scale, the northeast (NE) monsoon period shows a distinct difference in the widespread  
403 intensity of TSS distribution as compared to the southwest (SW) monsoon period, along the Sarawak  
404 coastline over the 17 years of the considered time series (Fig. 7). Mapping of temporal variations  
405 between monsoons using time-series MODIS-Aqua datasets can provide an improved understanding  
406 on the intensity of monsoonal patterns in driving the TSS distribution in this region. As shown in Figure  
407 7, TSS release can be seen to extend further into the open ocean South China Sea region during the  
408 NE monsoon periods (Fig. 7a) in comparison to the SW monsoon periods (Fig. 7b).

409 In addition, the differences in TSS release between the NE and SW monsoons  $((NE-SW)/NE \times 100)$  were  
410 mapped as shown in Fig. 7c. Widespread TSS plumes are detected at Lundu/Sematan region (>80 %  
411 relative difference in TSS concentration) on the southwest side of the study area, while substantial  
412 TSS plumes are observed in front of the Igan river channel, with more than 50 % relative difference in  
413 TSS concentration in comparison to SW monsoon periods. Sadong coastal area is observed to receive  
414 considerable TSS loadings (> 30%) during NE monsoon periods.

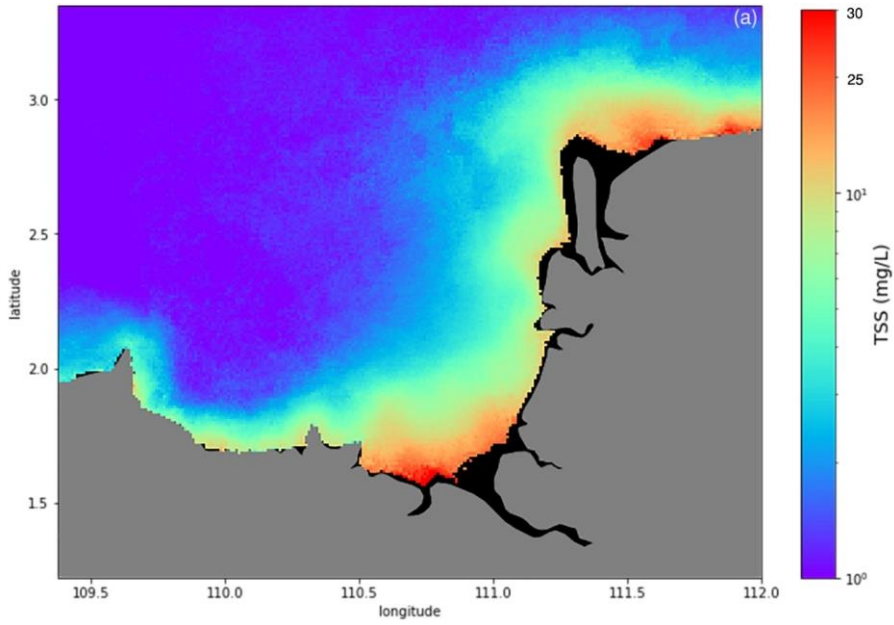
415 These coastal areas would thus be more likely to be impacted by the TSS release during the NE  
416 monsoon periods. These findings further strengthen the evidence that tropical rivers are majorly  
417 impacted by climatic variability such as monsoonal patterns, as highlighted in a study at Baleh river in  
418 Sarawak (Chong et al., 2021). This suggests that monsoon rains, which typically last for several months,  
419 play an integral role in driving the discharge of TSS in tropical rivers.

420

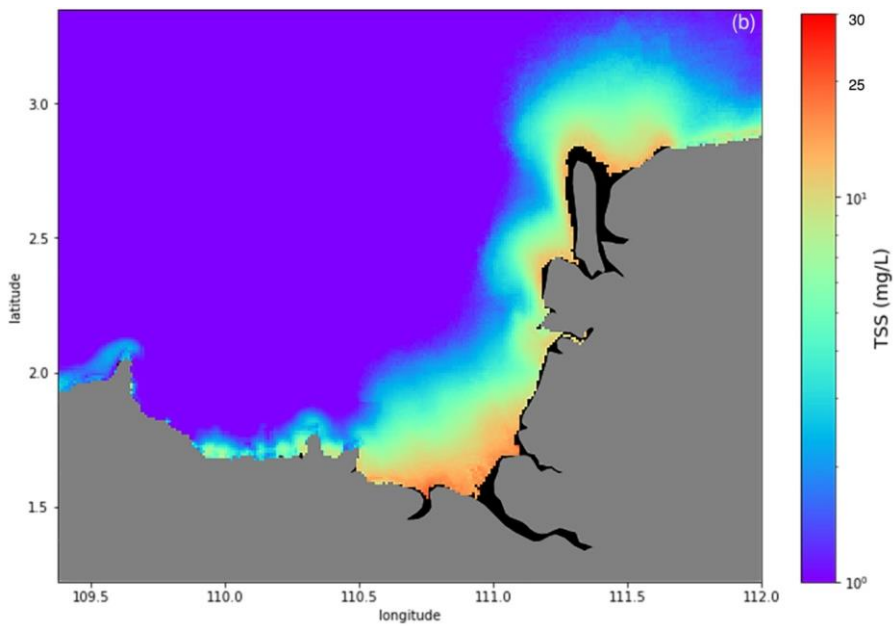
421

422

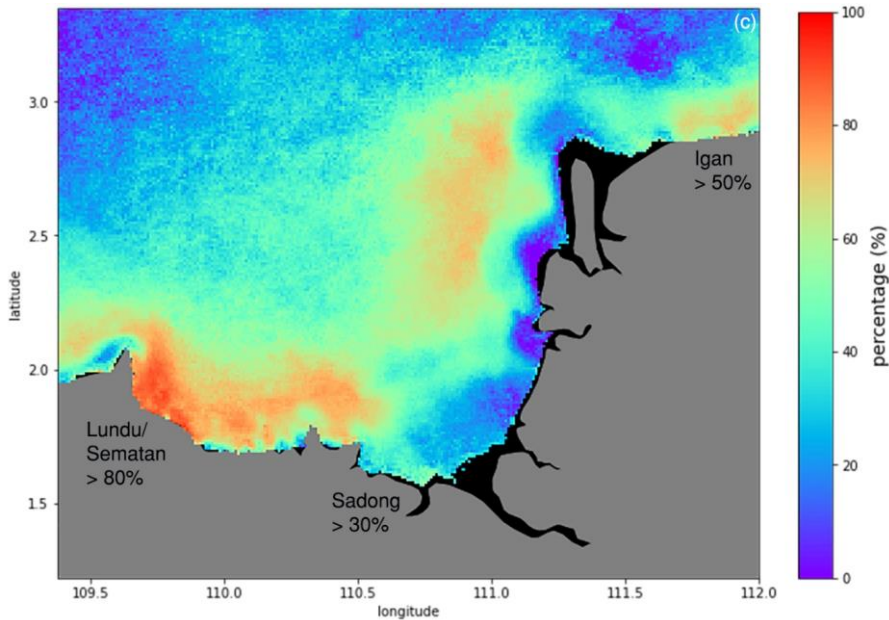
423



424



425



426  
 427 Fig. 7: Long-term average of TSS estimates (mg/L) during the Northeast monsoon (a), and the Southwest monsoon (b). The  
 428 map of TSS difference between the Northeast and Southwest monsoon periods, computed in relative percentage (%), is  
 429 shown in (c).

430 Several climatic studies in the Borneo region highlighted 2009 as a year with extreme rainfall events  
 431 which caused major floods in Sarawak (Dindang et al., 2011; Sa'adi et al., 2017), while drought events  
 432 were reported in 2014 (Bong and Richard, 2020). Hence, in this study, TSS dynamics for the Lupar and  
 433 Rajang rivers were studied by assessing the variation of TSS values at selected pixels in relation to  
 434 monsoonal rainfall patterns in 2009 and 2014 (Supplementary Materials; Fig. S3).

435 ~~Monthly precipitation values (mm) over the Lupar and Rajang basins were extracted from the Global~~  
 436 ~~Precipitation Measurement (GPM) satellite datasets (Supplementary Materials, Fig. S4 – 7) in order to~~  
 437 ~~assess the influence of precipitation in each river basin in relation to TSS concentration at the~~  
 438 ~~corresponding river mouth.~~

439 Generally, the results show fluctuations of TSS concentrations across the NE and SW monsoon periods  
 440 in relation to precipitation values (Fig. 8a – d). Based on Fig. 8a, monthly precipitation values recorded

441 for the Lupar river basin in 2009 showed a clear decreasing trend from the NE monsoon period (wet  
442 season) to the SW monsoon period (dry season), while gradually increasing approaching the year end's  
443 NE monsoonal period. A similar precipitation pattern was observed for the Rajang river basin during  
444 the same year (Fig. 8c).

445 However, these results also show that the TSS distribution (mg/L) at the Lupar river mouth seems to  
446 show no distinct trend of decreasing TSS concentration estimates during the SW monsoon period in  
447 year 2009 (Fig. 8a) in relation to its precipitation values. Additionally, a sharp rise of TSS release can  
448 be seen in the month of May (beginning of SW monsoon period), with a near equivalent intensity of  
449 TSS release during the NE monsoon period. This observation may potentially be caused by the lag  
450 between the time of rainfall events occurring during NE monsoon periods and TSS release entering  
451 the coastal river regions. A similar observation was described by Sun et al. (2017a) suggesting that  
452 riverine outputs could take several days, and even up to one month to reach the coastal river points.  
453 Considering the occurrence of extreme rainfall events in 2009, our findings are in agreement with  
454 these processes as TSS concentrations generally exhibit a similar intensity throughout the NE and SW  
455 monsoonal periods for the Lupar river (Fig. 8a). This result could suggest that the occurrence of  
456 extreme rainfall events, as reported for the year 2009, can exert a much larger impact on TSS  
457 transportation and release in monsoon-driven tropical rivers.

458 ~~However, our estimates show a generally lower TSS concentration at the Rajang river mouth during~~  
459 ~~the SW monsoon periods (dry season) in 2009 (Fig. 8c) as compared to the Lupar river mouth (Fig. 8a).~~  
460 ~~While these observations were recorded during the same year in 2009, when Sarawak experienced~~  
461 ~~extreme rainfall events, the monsoonal influence between these two different river basins show a~~  
462 ~~slight difference in terms of TSS distribution. A possible reason for these observations can be explained~~  
463 ~~by the Rajang river's unique meandering features, which can potentially induce a different~~  
464 ~~sedimentological behaviour compared to the Lupar river channels, which was discussed by Omorinoye~~

465 ~~et al. (2021) in a study on geomorphological features of the Sadong river in relation to the~~  
466 ~~sedimentation process.~~

467 Drought events in 2014 can be seen to impact the precipitation values at both the Lupar (Fig. 8b) and  
468 Rajang river basins (Fig. 8d). There is no apparent patterns of decreasing precipitation values during  
469 the shift of NE to SW monsoonal periods as compared to the year 2009, for either river basin. However,  
470 precipitation values were found to increase sharply during the year end NE monsoon period for both  
471 river basins. The TSS concentrations at the Lupar coastal river points were found to be the highest  
472 during the NE monsoon period earlier in January and February of 2014 (Fig. 8b). This may be due to  
473 the temporal lag in the transition of TSS discharge into the coastal systems arising from the prior  
474 months (November and December) in the previous year, when higher rainfall events were typically  
475 observed in this region (Gomyo and Koichiro, 2009; Tangang et al., 2012). The TSS distribution at both  
476 Lupar and Rajang coastal river points showed no distinct trend in relation to the precipitation values  
477 throughout a period of ten months until November 2014. These findings suggest that coastal areas in  
478 the Borneo region may not be experiencing critical water quality degradation during dry seasons.

479

480

481

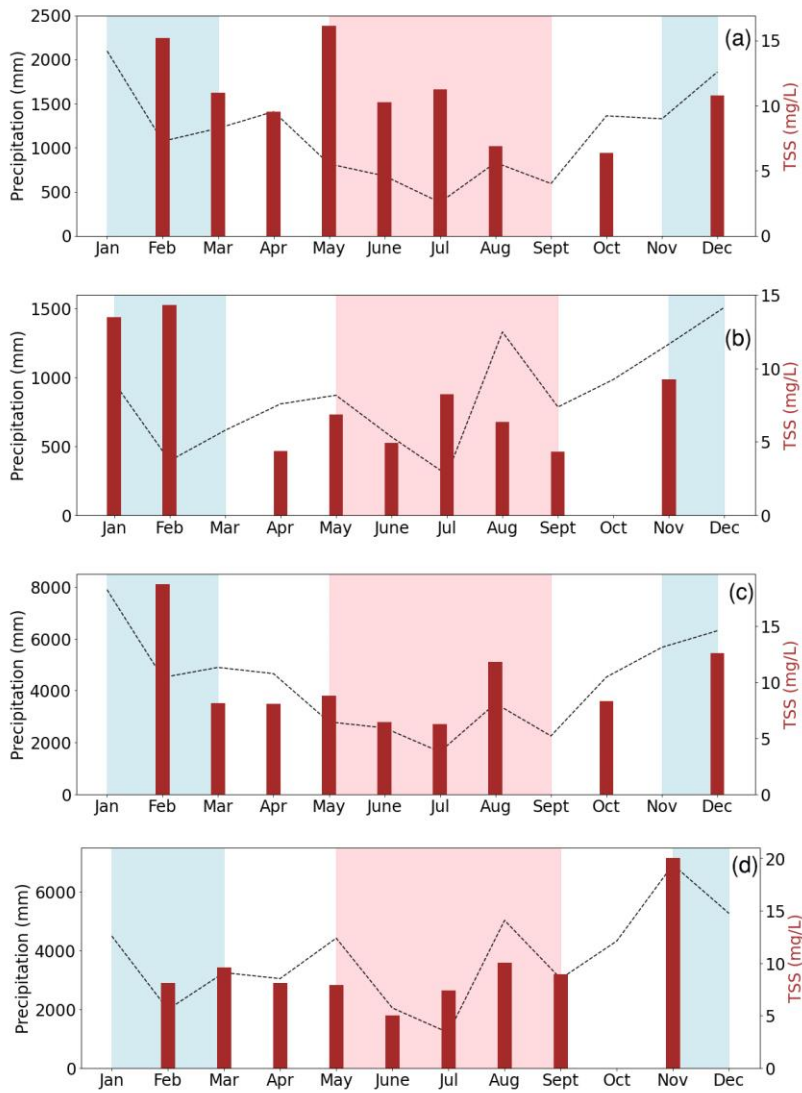
482

483

484

485

486



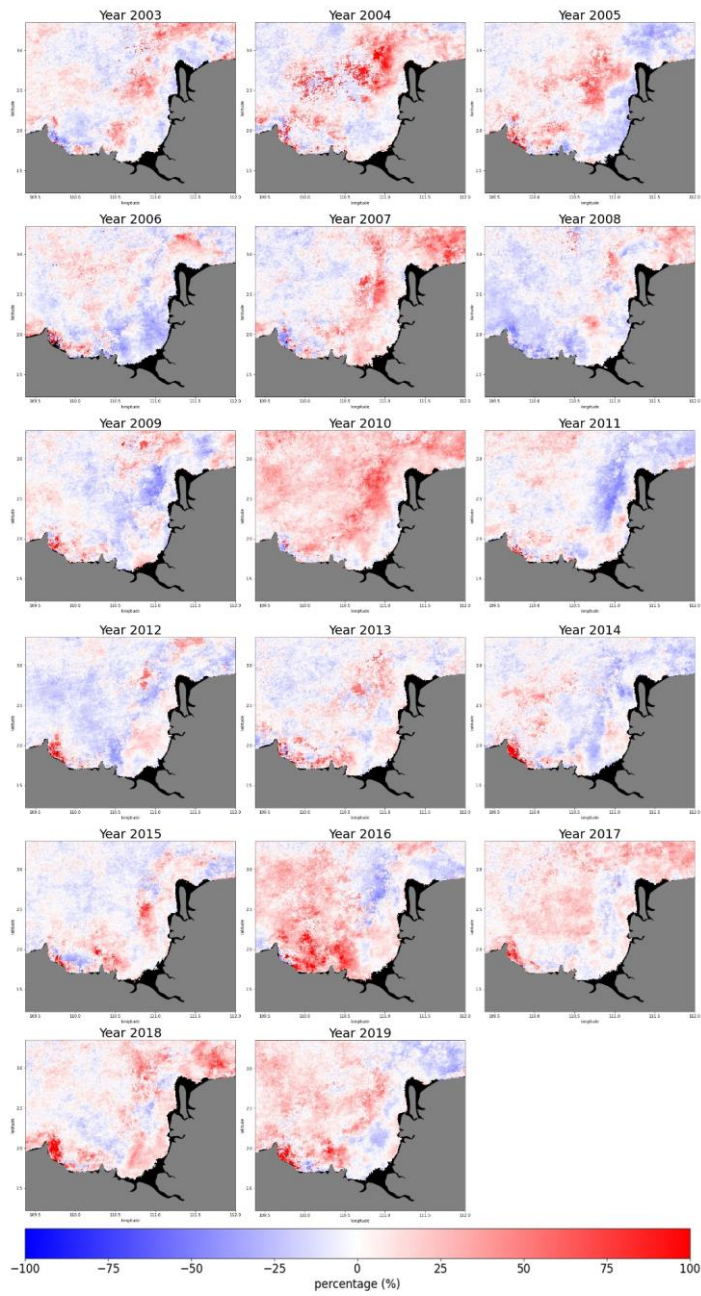
487  
 488 Fig. 8: Temporal analysis of precipitation (mm) from the Lupar and Rajang river basins in relation to TSS concentrations (mg/L)  
 489 during the NE and SW monsoon periods at the Lupar ((a): 2009; (c): 2014) and Rajang ((b): 2009; (d): 2014) coastal river point.  
 490 The NE monsoon months are highlighted with a blue background; those of the SW monsoon with a pink background, and  
 491 intermonsoon periods with a white background.



### 3.2.1 Temporal TSS anomalies

Considering the temporal variation recorded across monsoons, maps of relative TSS anomalies were calculated for each year as the difference with respect to the long-term TSS mean (Fig. 5), in order to detect changes of TSS distribution occurring annually (Fig. 9). As shown in Figure 9, year 2010 experienced a distinct increase of TSS distribution (approximately 100 %), with widespread pattern extending into open ocean waters, in comparison to the long-term TSS mean. This finding provides an interesting insight into the effects of extreme rainfall events as recorded in year 2009, which could potentially intensify TSS release into the coastal and open ocean waters. The effects of TSS release can still be seen a year after the extreme rainfall events in this region. This observation could provide further evidence that the impacts of the TSS release from the land into rivers and coastal systems may only take effect after a substantial period, as previously observed by Sun et al. (2017a).

Figure 9 further reveals an interesting pattern of TSS increase in the Samunsam-Sematan region from year 2004 until 2019, with exceptions during the years 2007 and 2008. As previously highlighted in Section 3.1, the Samunsam-Sematan region has been observed to be a vulnerable coastal area with respect to TSS water quality degradation. From the annual map of TSS anomalies (Fig. 9), we can see that the TSS distribution has the tendency to accumulate in the Samunsam-Sematan region, as opposed to being distributed into the open ocean waters. This may be due to the geographical and hydrological characteristics of these coastal regions (Martin et al., 2018), as the TSS release may be sheltered from open ocean waters, and hence induce a higher TSS accumulation in these coastal regions.



517

518 Fig. 9: Map of relative TSS distribution anomalies with respect to the long-term mean, represented as percentage (%), from  
 519 year 2003 until 2019.

520 3.3 Hydrological factors driving TSS discharge

521 Apart from the influence of monsoonal patterns, hydrological factors such as the river discharge are  
522 among the dominant drivers in transporting various water constituents in riverine and coastal systems  
523 (Loisel et al., 2014; Petus et al., 2014; Sun, 2017b; Verschelling et al., 2017). In this study, river  
524 discharge from the Lupar and Rajang basins was estimated and investigated.

525 Yearly river discharge estimates from 2003 until 2019 were investigated to assess its effect on the TSS  
526 distribution (Fig. 10) represented by changes in TSS values for pixels located at each Lupar and Rajang  
527 coastal river points (Supplementary Materials, Fig. S3). Figure 10a shows that river discharge values in  
528 the Lupar basin (750 to 1050 m<sup>3</sup>/s) are approximately twice lower than the Rajang river discharge (Fig.  
529 10b), which recorded a range of 3,200 to 4,000 m<sup>3</sup>/s.



531  
532 Fig. 10: Time-series analysis of river discharge (m<sup>3</sup>/s) in relation to TSS concentrations (mg/L) for the Lupar (a) and Rajang (b)  
533 basins from year 2003 to 2019. Note the differing scaling on the ordinate axes in each plot.

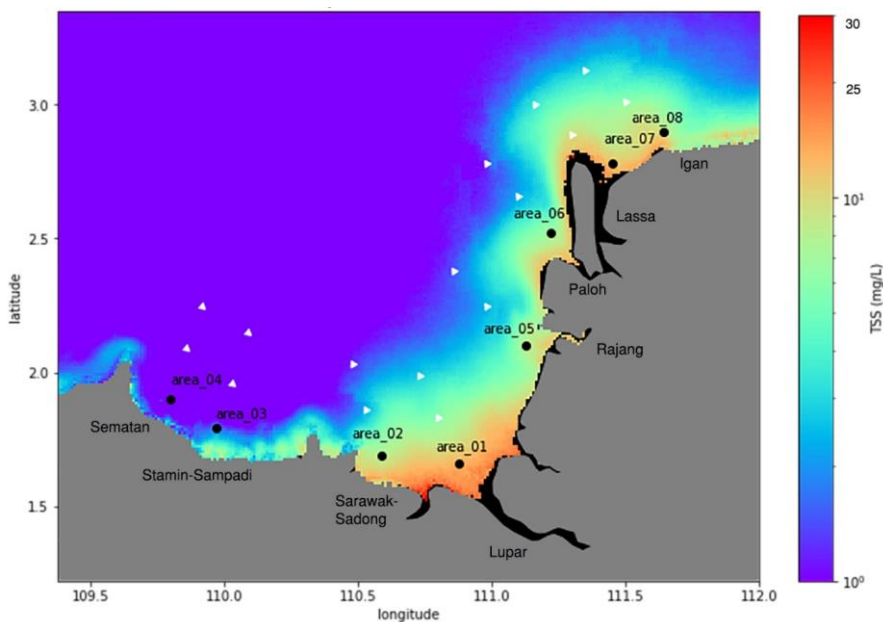
534 ~~From our findings,~~ discrepancies between TSS estimates and river discharge were identified in both  
535 the Lupar and Rajang coastal regions in these annual time-series, where river discharge was inversely  
536 correlated with TSS estimates. These discrepancies are not uncommon, as previously highlighted in a  
537 study by Zhan et al. (2019). Especially in 2010 for the Lupar river, Fig. 10a shows a drop in TSS release  
538 in relation to the steady increase of river discharge from the river basin. In 2011 and 2012, a negative  
539 correlation can be seen between river discharge and TSS estimates, while in subsequent years from  
540 2013 until 2015, there is a clear positive correlation. Although there is no obvious environmental  
541 factor that would explain these discrepancies, these findings may imply a complex interaction  
542 between human interventions, such as damming and deforestation activities, as well as varying  
543 hydrological and atmospheric conditions (wind and tidal mixing) in regulating TSS dynamics (Wu et al.,  
544 2012; Zhan et al., 2019).

545 The correlation between TSS release and river discharge at both the Lupar and Rajang coastal areas  
546 was further evaluated in this study. Even though river discharge has been shown (in other global  
547 studies) to be one of the dominant factors in moderating TSS release (Fabricius et al., 2016; Tilburg et  
548 al., 2015; Verschelling et al., 2017; Wu et al., 2012), the TSS distribution at both the Lupar and Rajang  
549 river mouths in this study can be seen to be only poorly correlated with river discharge from each river  
550 basin (Supplementary Materials, Fig. S8a and b). The TSS output from the Lupar basin recorded a  
551 correlation coefficient of  $r = 0.15$ , while river discharge from the Rajang basin did not substantially  
552 influence the TSS release either, with  $r = 0.27$  throughout the seasons. Coupled with tidal mixing  
553 processes (Ramaswamy et al., 2004; Zhou et al., 2020), it is possible that human activities such as  
554 deforestation, logging, and construction of dams, which are largely occurring within the Rajang basin  
555 (Alamgir et al., 2020), are mainly driving TSS release and resuspension in this area. This indicates that  
556 although TSS release is regarded to be highly dependent on, and controlled by river discharge patterns,  
557 this interaction often represents an intricate process linked to local hydrodynamics process and socio-  
558 economic conditions (Espinoza Villar et al., 2013; Fabricius et al., 2016; Valerio et al., 2018; Zhan et al.,  
559 2019).

560 3.4 Variability of TSS across coastal waters

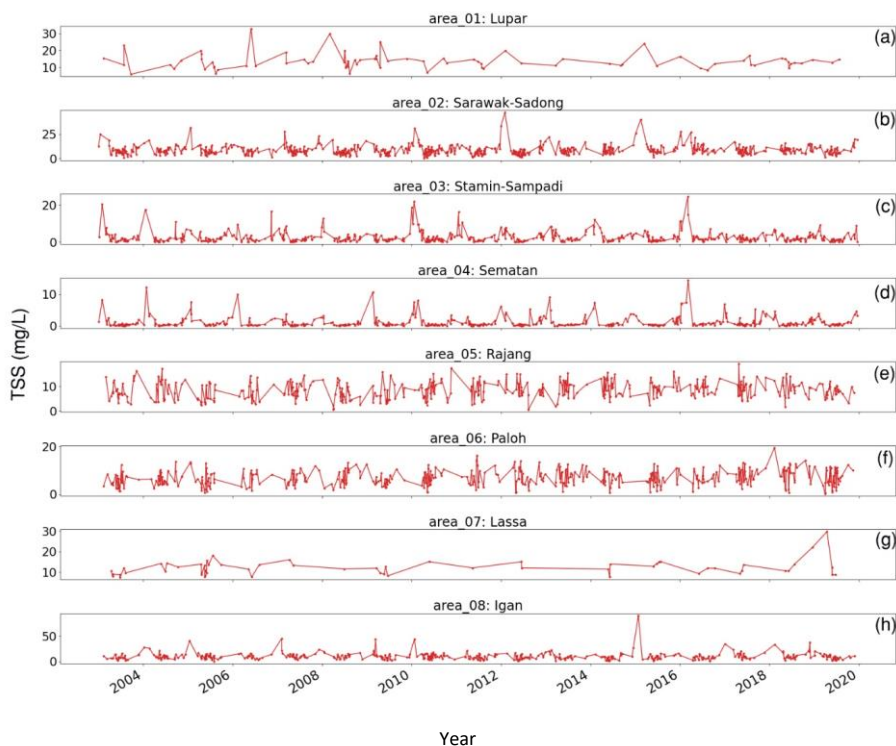
561 As previously observed in Fig. 5, varying river plumes of TSS were evidently detected within the coastal  
562 regions of the study area. Notably, coastal river plumes represent important factors driving the  
563 transport of water constituents and nutrients from coastlines to the open oceanic systems (Petus et  
564 al., 2014). To assess this and evaluate the water quality status in coastal zones, the spatial extent of  
565 TSS release was investigated along transects covering the territorial (12 nautical miles) and open water  
566 areas (24 nautical miles) of the Sarawak region (Fig. 11).

567 A total of eight coastal points were selected based on the main river mouths located in the southwest  
568 region of Sarawak. Transect points are positioned in a line starting at the coastal river points to  
569 examine the variations of TSS distribution across different water zones. Daily changes in TSS  
570 concentration for each pixel located in front of the river mouths were plotted from 2003 until 2019  
571 (Fig. 12).



572

573 Fig. 11: Map of average TSS estimates (mg/L) with indicators at eight main river mouths and their transect, extending from  
 574 coastal waters into territorial and open ocean systems. Indicators of each river mouths are as follows: area\_01 – Lupar river;  
 575 area\_02 – Sarawak-Sadong river; area\_03 - Stamin-Sampadi river i; area\_04 – Sematan river; area\_05: Rajang river; area\_06:  
 576 Paloh river; area\_07: Lassa river; and area\_08: Igan river).



577  
 578 Fig. 12: Graphs of daily TSS estimates (mg/L) recorded at eight river mouth points from 2003 to 2019. Presentation of each  
 579 river mouths is as follows: a) area\_01; b) area\_02; c) area\_03; d) area\_04; e) area\_05; f) area\_06; g) area\_07; h) area\_08.  
 580 Note the different TSS scales in each plot.

581 From the high temporal resolution graphs in Fig. 12, no general trend of TSS concentration can be  
 582 identified over the years at each coastal point. It is worth highlighting that the daily temporal  
 583 resolution was particularly affected at coastal points located in front of the Lupar (area\_01) and Lassa  
 584 (area\_07) river mouths due to various pixel data quality issues in these areas. Nonetheless, more than  
 585 80 satellite images with minimum cloud coverage at these two locations were processed, while the  
 586 remaining coastal points had a total of more than 400 satellite images to assess the temporal trend.

587 Despite the fact that no distinct upward or downward trend was observed, our findings indicate that  
588 several river mouths are actively discharging and accumulating substantial TSS amounts over the  
589 period of years, while resuspension of bottom sediments induced by wind and tidal cycle is another  
590 factor contributing to the variation of TSS values (Park, 2007; Song et al., 2020).

591 The coastal region of the Sarawak-Sadong river (area\_02) shows relatively high TSS distribution  
592 patterns with some periods recording an estimate of over 30 mg/L of TSS concentration. This is in  
593 agreement with the localised characteristics of the Sarawak river basin which essentially drains  
594 through the populated Kuching area with high industrial and development activities in the capital city  
595 of Sarawak (DID, 2021b). In comparison with other river mouth points, a steady TSS concentration  
596 below 20 mg/L was recorded across the Stamin-Sampadi (area\_03), Sematan (area\_04), Rajang  
597 (area\_05), and Paloh (area\_06) river mouths. Consistently high TSS values in the daily plots were  
598 recorded at the Lupar (area\_01) and Pulau Bruit-Lassa (area\_07) river mouths, with estimates of up to  
599 30 mg/L on a near-daily basis. Similar high TSS amounts from the Igan (area\_08) river mouth, situated  
600 northeast side of the Pulau Bruit-Lassa region, were observed in Cherukuru et al. (2021) and Staub et  
601 al. (2000).

602 Although the daily TSS estimates at each river point are in line with various reported studies (Chen et  
603 al., 2011, 2015b; Kim et al., 2017; Mengen et al., 2020; Zhang et al., 2010a), these estimates can be  
604 expected to be much higher for sampling points much closer to the river mouths. The selection of  
605 coastal river points in this study was made to minimize the gaps with respect to various pixel data  
606 quality issues in the MODIS-Aqua datasets, and hence, the use of coastal river points closer to shore  
607 would have been impractical.

608 These findings further suggest that higher TSS loadings within the coastal river areas would have been  
609 diluted or deposited while travelling to the open oceanic systems as they are weakly impacted by river  
610 discharge in relation to offshore distance (Espinoza Villar et al., 2013). This understanding can be  
611 observed in Fig. 13, which shows a progressively decreasing TSS estimates at each transect in relation

612 to the distance from the shore. Generally, TSS estimates in coastal zones (first transect point) show  
613 considerably higher TSS concentrations. When moving outwards to territorial waters (second transect  
614 point), TSS concentration estimates decrease by nearly 50 % before travelling to open ocean systems  
615 (third transect point), except for the northeast regions (area\_07 and area\_08) which seem to show  
616 large extension of TSS plumes to the open ocean waters, as also highlighted by Cherukuru et al. (2021).  
617 A reversed trend can be seen in the plot corresponding to the Sematan coastal river systems, although  
618 the absolute increase in TSS estimates across water zones (0.2 mg/L in total) here is only marginal (Fig.  
619 135d).

~~620 Nonetheless, it is important to present these synoptic findings to address existing water quality  
621 practices and regulations implemented in this local region, in order to improve the monitoring and  
622 management of its coastal systems. According to the Malaysia Marine Water Quality Criteria and  
623 Standard (Supplementary Materials, Table S2), the coastal areas of Sarawak are dominantly  
624 categorised as Class I quality. Our findings in the southwest coastal areas (Sematan and Stamin-  
625 Sampadi) showed that the coral reefs there can be well-maintained with negligible impacts from TSS  
626 loadings (Fig. 11). While these Sematan and Stamin-Sampadi coasts can be seen to be in a healthy  
627 water quality state (low average TSS concentration, see e.g. Fig 11), the high coefficient variation  
628 reported in these coastal waters, as previously highlighted in Section 3.1 (Fig. 6), clearly stresses the  
629 importance of understanding how the quality of coastal systems can vary and be affected by human  
630 intervention and changing landscapes over time.~~

631

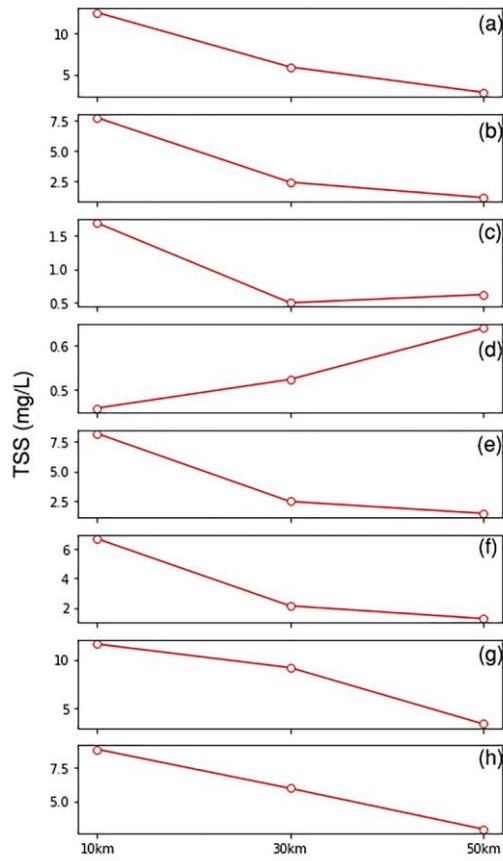
632

633

634

635





636

637 Fig. 13: Average TSS estimates (mg/L) computed from 2003 to 2019 for each of the eight rivers (area\_01: (a), area\_02: (b);  
 638 area\_03: (c); area\_04: (d); area\_05: (e); area\_06: (f); area\_07: (g); and area\_08: (h)) and their relevant transect points with  
 639 distance of 10 km (coastal waters), 30 km (territorial waters) and 50 km (open ocean waters) from the shoreline. Note the  
 640 varying TSS scales on the ordinate axes in each plot.

641

642

643

644

645 3.5 Discussion of TSS implications for coastal waters

646 High discharge of TSS into coastal environments can lead to adverse environmental and ecological  
647 implications. The presence of TSS affects water transparency and light availability within the surface  
648 waters (Dogliotti et al., 2015; Nazirova et al., 2021; Wang et al., 2021). Among others, TSS affects the  
649 photosynthesis activities of algae and macrophytes. TSS in water creates a reduction in light  
650 penetration, which impacts the primary production of aquatic organisms and hence the support  
651 system of marine life (Bilotta and Brazier, 2008; Loisel et al., 2014).

652 Additionally, TSS exerts an influence on zooplankton communities. Reduction in water clarity induces  
653 changes in the zooplankton's biomass volume and composition, while TSS may carry a level of toxicity  
654 which affects zooplankton through ingestion (Chapman et al., 2017; Donohue and Garcia Molinos,  
655 2009). Apart from that, accumulation and deposition of sediments decreases the level of dissolved  
656 oxygen (DO) at the bottom of the water column, and subsequently impacts the benthic invertebrate  
657 groups (Chapman et al., 2017). Moreover, substantial TSS deposition tends to cause harmful physical  
658 effects to these benthic groups, such as abrasion, and even clogging by sediment particles (Chapman  
659 et al., 2017; Langer, 1980).

660 As a result of these TSS effects on lower trophic levels, fish communities are critically impacted, with  
661 a reduction in diversity and abundance (Kemp et al., 2011). While fish communities learn to adapt to  
662 a range of TSS loads (Macklin et al., 2010), increase of TSS concentrations often depletes DO  
663 concentrations in the water system and causes stress towards these aquatic communities (Henley et  
664 al., 2000). Fish populations tend to decrease, as feeding and growth rates are negatively impacted  
665 (Shaw and Richardson, 2001; Sutherland and Meyer, 2007).

666 Threats to coral reefs have been linked to sediment-induced stress which often leads to a reduction  
667 in the coral's growth and metabolic rate, as well as impending mortality (Erfteimeijer et al., 2012;  
668 Gilmour et al., 2006; Risk and Edinger, 2011). Factors of coral stress are driven by nutrient-rich  
669 sediments and microbes which are being carried by TSS, with impacts on the health of coral tissues

670 (Hodgson, 1990; Risk and Edinger, 2011; Weber et al., 2006). A reduction in light availability impedes  
671 the development of corals (Anthony and Hoegh-Guldberg, 2003; Rogers, 1979; Telesnicki and  
672 Goldberg, 1995). A combined increase in TSS and nutrient loadings contribute to the decrease of coral  
673 species diversity and composition (Fabricius, 2005).

674 Essentially, presence of TSS in water systems has impacts across various aquatic biota. With the severe  
675 implications of decreased fish population, this could lead to a disruption of fisheries activities by local  
676 communities, especially considering that more than 80 % of the Sarawak population is living in the  
677 coastal areas (DID, 2021a). Coral reefs are important coastal biodiversity assets to the Sarawak region,  
678 especially around the Talang-Talang and Satang islands on the southwest coast of Sarawak (Long,  
679 2014). With the use of remote sensing technologies in monitoring Sarawak coastal water quality, the  
680 approach presented in this paper provides digital-based solutions to assist relevant authorities and  
681 local agencies to better manage the Sarawak coastal waters and their resources.

682

683

684

685

686

687

688

689

690

691

692

693

694

695

#### 696 4.0 Conclusion

697 In this study, a regional empirical TSS retrieval model was developed to analyse TSS dynamics along  
698 the southwest coast of Sarawak. The empirical relationship between in situ reflectance values,  $Rrs(\lambda)$ ,  
699 and in situ TSS concentrations was established using a green-to-red band ratio using the MODIS-Aqua  
700  $Rrs(530)$  and  $Rrs(666)$  reflectance bands. An evaluation of the TSS retrieval model was carried out with  
701 error metric assessment, which yielded results of bias = 1.0, MAE = 1.47 and RMSE = 0.22 in mg/L  
702 computed in log<sub>10</sub>-transformed space prior to calculation. A statistical analysis using a k-fold cross  
703 validation technique (k = 7) reported a low error metrics (RMSE = 0.2159, MAE = 0.1747).

704 The spatial TSS distribution map shows widespread TSS plumes detected particularly in the Lupar and  
705 Rajang coastal areas, with average TSS range of 15 – 20 mg/L estimated at these coastal areas. Based  
706 on the spatial map of the TSS coefficient of variation, large TSS variability was identified in the  
707 Samunsam-Sematan coastal areas (CV > 90 %). The map of temporal variation of TSS distribution  
708 points to a strong monsoonal influence in driving TSS release, with large differences identified  
709 between the northeast and southwest monsoon periods in this region. From the annual TSS anomalies  
710 maps, the Samunsam-Sematan coastal areas demonstrated strong TSS variation spatially, while  
711 widespread TSS distribution with nearly 100 % of TSS increase in comparison to long term mean was  
712 observed in 2010. Furthermore, our study on river discharge in relation to TSS release demonstrated  
713 a weak relationship at both the Lupar and Rajang coastal river points. Study on the TSS variability  
714 across coastal river mouths implied that higher TSS loadings in the coastal areas are potentially being  
715 deposited or diluted in the process of being transported into the open ocean waters, with varying  
716 magnitude at several coastal river points.

717 Overall, these ~~coastal zones remain within local water quality standards to support various marine and~~  
718 ~~socio-economic activities in this region.~~ coastal areas of Sarawak are dominantly categorised as Class  
719 I quality, which remain within local quality standards to support various marine and socio-economic  
720 activities in this region. Our findings in the southwest coastal areas (Sematan and Stamin-Sampadi)

721 [showed that the coral reefs there can be well-maintained with negligible impacts from TSS loadings.](#)

722 However, it is important to highlight the various human activities that are widely ongoing in this  
723 region, which include deforestation and logging activities (Alamgir et al., 2020; Hon and Shibata, 2013;  
724 Vijith et al., 2018). Impacts from these activities in Sarawak can potentially aggravate current soil  
725 erosion issues, and ultimately induce more soil leaching and runoff from land to water systems,  
726 especially during heavy rainfall events (Ling et al., 2016; Vijith et al., 2018). As a result, human activities  
727 may have a greater influence on driving riverine sediments than climatological factors, as reported by  
728 Song et al. (2016). As such, this work presents the first observation of TSS distributions at large spatial  
729 and temporal scales in Sarawak's coastal systems, and of the potential associated impacts on the  
730 South China Sea. The findings derived from this work can be used to support local authorities in  
731 assessing TSS water quality status in the coastal areas of concern, and to enhance coastal management  
732 and conservation strategies. The application of remote sensing technologies is of great benefit in the  
733 development of sustainable sediment management in the Sarawak coastal region, as demonstrated  
734 in this study.

735 Data availability. The dataset related to this study is available as supplement to this paper.

736 Author contributions. Conceptualization, J.C., N.C., E.L., and M.M.; Formal analysis, J.C., N.C. and E.L.;  
737 Funding acquisition, M.M, N.C., and A.M.; Investigation, J.C., N.C., E.L, M.P., P.M., A.M., and M.M.;  
738 Methodology, J.C., N.C., E.L., and M.M.; Resources, J.C., N.C., E.L, M.P., and M.M.; Validation, J.C.,  
739 N.C., E.L. and M.M.; Writing— original draft, J.C.; Writing—review & editing, J.C., N.C., E.L, P.M., and  
740 M.M.; Supervision, M.M., N.C., and A.M.; Project administration, M.M., A.M., and N.C.

741 Competing interests. The authors declare that they have no conflict of interest.

742 Acknowledgement. We thank Sarawak Forestry Department and Sarawak Biodiversity Centre for  
743 permission to conduct collaborative research in Sarawak under permit numbers NPW.907.4.4(Jld.14)-  
744 161, SBC-RA-0097-MM, and Park Permit WL83/2017. We would like to extend our gratitude to all the  
745 boatmen and crew during all the field expeditions. Special thanks to Pak Mat and Minhad during the

746 western region sampling, and Captain Juble, as well as Lukas Chin, during the eastern region cruises.  
747 We are appreciative to members of AQUES MY for their kind participation and involvement, especially  
748 to Ashleen Tan, Jack Sim, Florina Richard, Faith Chaya, Edwin Sia, Faddrine Jang, Gonzalo Carrasco,  
749 Akhmetzada Kargazhanov, Noor Iskandar Noor Azhar, and Fakharuddin Muhamad. The study was  
750 supported by Australian Academy of Sciences under the Regional Collaborations Programme, Sarawak  
751 Multimedia Authority (Sarawak Digital Centre of Excellence) and Swinburne University of Technology  
752 (Swinburne Research Studentship).

753

754

755

756

757

758

759

760

761

762

763

764

765

766

767

768

769

770

771

772

773

774

775

776 References:

- 777 Ahn, Y. and Shanmugam, P.: Derivation and analysis of the fluorescence algorithms to estimate  
778 phytoplankton pigment concentrations in optically, , doi:10.1088/1464-4258/9/4/008, 2007.
- 779 Alamgir, M., Campbell, M. J., Sloan, S., Engert, J., Word, J. and Laurance, W. F.: Emerging challenges  
780 for sustainable development and forest conservation in Sarawak, Borneo, PLoS One, 15(3), 1–20,  
781 doi:10.1371/journal.pone.0229614, 2020.
- 782 Alcântara, E., Bernardo, N., Watanabe, F., Rodrigues, T., Rotta, L., Carmo, A., Shimabukuro, M.,  
783 Gonçalves, S. and Imai, N.: Estimating the CDOM absorption coefficient in tropical inland waters  
784 using OLI/Landsat-8 images, Remote Sens. Lett., 7(7), 661–670,  
785 doi:10.1080/2150704X.2016.1177242, 2016.
- 786 Anthony, K. R. N. and Hoegh-Guldberg, O.: Kinetics of photoacclimation in corals, *Oecologia*, 134(1),  
787 23–31, doi:10.1007/s00442-002-1095-1, 2003.
- 788 Babin, M., Stramski, D., Ferrari, G. M., Claustre, H., Bricaud, A., Obolensky, G. and Hoepffner, N.:  
789 Variations in the light absorption coefficients of phytoplankton , nonalgal particles , and dissolved  
790 organic matter in coastal waters around Europe, , 108, doi:10.1029/2001JC000882, 2003.
- 791 Bailey, S. W., Franz, B. A. and Werdell, P. J.: Estimation of near-infrared water-leaving reflectance for  
792 satellite ocean color data processing, *Opt. Express*, 18(7), 7521, doi:10.1364/oe.18.007521, 2010.
- 793 Balasubramanian, S. V., Pahlevan, N., Smith, B., Binding, C., Schalles, J., Loisel, H., Gurlin, D., Greb, S.,  
794 Alikas, K., Randla, M., Bunkei, M., Moses, W., Nguyễn, H., Lehmann, M. K., O'Donnell, D., Ondrusek,  
795 M., Han, T. H., Fichot, C. G., Moore, T. and Boss, E.: Robust algorithm for estimating total suspended  
796 solids (TSS) in inland and nearshore coastal waters, *Remote Sens. Environ.*, 246(February), 111768,  
797 doi:10.1016/j.rse.2020.111768, 2020.
- 798 Bhardwaj, J., Gupta, K. K. and Gupta, R.: A review of emerging trends on water quality measurement  
799 sensors, *Proc. - Int. Conf. Technol. Sustain. Dev. ICTSD 2015*, (April), 1–6,  
800 doi:10.1109/ICTSD.2015.7095919, 2015.
- 801 Bilotta, G. S. and Brazier, R. E.: Understanding the influence of suspended solids on water quality and  
802 aquatic biota, *Water Res.*, 42(12), 2849–2861, doi:10.1016/j.watres.2008.03.018, 2008.
- 803 Bong, C. H. J. and Richard, J.: Drought and climate change assessment using standardized  
804 precipitation index (Spi) for sarawak river basin, *J. Water Clim. Chang.*, 11(4), 956–965,  
805 doi:10.2166/wcc.2019.036, 2020.
- 806 Cao, F., Tzortziou, M., Hu, C., Mannino, A., Fichot, C. G., Del Vecchio, R., Najjar, R. G. and Novak, M.:  
807 Remote sensing retrievals of colored dissolved organic matter and dissolved organic carbon  
808 dynamics in North American estuaries and their margins, *Remote Sens. Environ.*, 205(November  
809 2017), 151–165, doi:10.1016/j.rse.2017.11.014, 2018.
- 810 Chapman, P. M., Hayward, A. and Faithful, J.: Total Suspended Solids Effects on Freshwater Lake  
811 Biota Other than Fish, *Bull. Environ. Contam. Toxicol.*, 99(4), 423–427, doi:10.1007/s00128-017-  
812 2154-y, 2017.
- 813 Chen, S., Huang, W., Chen, W. and Chen, X.: An enhanced MODIS remote sensing model for  
814 detecting rainfall effects on sediment plume in the coastal waters of Apalachicola Bay, *Mar. Environ.  
815 Res.*, 72(5), 265–272, doi:10.1016/j.marenvres.2011.09.014, 2011.
- 816 Chen, S., Han, L., Chen, X., Li, D., Sun, L. and Li, Y.: Estimating wide range Total Suspended Solids  
817 concentrations from MODIS 250-m imageries: An improved method, *ISPRS J. Photogramm. Remote  
818 Sens.*, 99, 58–69, doi:10.1016/j.isprsjprs.2014.10.006, 2015a.

819 Chen, S., Han, L., Chen, X., Li, D., Sun, L. and Li, Y.: Estimating wide range Total Suspended Solids  
820 concentrations from MODIS 250-m imageries: An improved method, *ISPRS J. Photogramm. Remote*  
821 *Sens.*, 99, 58–69, doi:10.1016/j.isprsjprs.2014.10.006, 2015b.

822 Chen, Z., Hu, C. and Muller-karger, F.: Monitoring turbidity in Tampa Bay using MODIS / Aqua 250-m  
823 imagery, , 109, 207–220, doi:10.1016/j.rse.2006.12.019, 2007.

824 Cherukuru, N., Ford, P. W., Matear, R. J., Oubelkheir, K., Clementson, L. A., Suber, K. and Steven, A.  
825 D. L.: Estimating dissolved organic carbon concentration in turbid coastal waters using optical  
826 remote sensing observations, *Int. J. Appl. Earth Obs. Geoinf.*, 52, 149–154,  
827 doi:10.1016/j.jag.2016.06.010, 2016a.

828 Cherukuru, N., Ford, P. W., Matear, R. J., Oubelkheir, K., Clementson, L. A., Suber, K. and Steven, A.  
829 D. L.: Estimating dissolved organic carbon concentration in turbid coastal waters using optical  
830 remote sensing observations, *Int. J. Appl. Earth Obs. Geoinf.*, 52, 149–154,  
831 doi:10.1016/j.jag.2016.06.010, 2016b.

832 Cherukuru, N., Martin, P., Sanwlan, N., Mujahid, A. and Müller, M.: A semi-analytical optical remote  
833 sensing model to estimate suspended sediment and dissolved organic carbon in tropical coastal  
834 waters influenced by peatland-draining river discharges off sarawak, borneo, *Remote Sens.*, 13(1), 1–  
835 31, doi:10.3390/rs13010099, 2021.

836 Chong, X. Y., Gibbins, C. N., Vericat, D., Batalla, R. J., Teo, F. Y. and Lee, K. S. P.: A framework for  
837 Hydrological characterisation to support Functional Flows (HyFFlow): Application to a tropical river,  
838 *J. Hydrol. Reg. Stud.*, 36(January), doi:10.1016/j.ejrh.2021.100838, 2021.

839 CIFOR: Forest Carbon Database, [online] Available from: <https://carbonstock.cifor.org/>, n.d.

840 Davies, J., Mathew, U., Aikanathan, S., Nyon, Y. C. and Chong, G.: A Quick Scan of Peatlands, *Wetl.*  
841 *Int. Malaysia*, 1(March), 1–80, 2010.

842 Department of Environment: Malaysia Marine Water Quality Standards and Index, , 16 [online]  
843 Available from: <https://www.doe.gov.my/portalv1/wp-content/uploads/2019/04/BOOKLET-BI.pdf>  
844 (Accessed 12 September 2021), 2019.

845 Department of Statistics, M.: Sarawak Population, *Popul. by Adm. Dist. Ethn. group, Sarawak, 2020*  
846 [online] Available from: [https://sarawak.gov.my/web/home/article\\_view/240/175](https://sarawak.gov.my/web/home/article_view/240/175), 2020.

847 DID: Department of Irrigation & Drainage Sarawak: Introduction to Integrated Coastal Zone  
848 Management, [online] Available from: [https://did.sarawak.gov.my/page-0-123-476-INTEGRATED-](https://did.sarawak.gov.my/page-0-123-476-INTEGRATED-COASTAL-ZONE-MANAGEMENT.html)  
849 [COASTAL-ZONE-MANAGEMENT.html](https://did.sarawak.gov.my/page-0-123-476-INTEGRATED-COASTAL-ZONE-MANAGEMENT.html) (Accessed 21 October 2021a), 2021.

850 DID: Department Of Irrigation & Drainage Sarawak, 2021b.

851 Dindang, A., Chung, C. N. and Seth, S.: Heavy Rainfall Episodes over Sarawak during January-February  
852 2011 Northeast Monsoon, *JMM Res. Publ.*, (11), 41, 2011.

853 Dogliotti, A. I., Ruddick, K. G., Nechad, B., Doxaran, D. and Knaeps, E.: A single algorithm to retrieve  
854 turbidity from remotely-sensed data in all coastal and estuarine waters, *Remote Sens. Environ.*, 156,  
855 157–168, doi:10.1016/j.rse.2014.09.020, 2015.

856 Donohue, I. and Garcia Molinos, J.: Impacts of increased sediment loads on the ecology of lakes, *Biol.*  
857 *Rev.*, 84(4), 517–531, doi:10.1111/j.1469-185X.2009.00081.x, 2009.

858 Erfemeijer, P. L. A., Riegl, B., Hoeksema, B. W. and Todd, P. A.: Environmental impacts of dredging  
859 and other sediment disturbances on corals: A review, *Mar. Pollut. Bull.*, 64(9), 1737–1765,  
860 doi:10.1016/j.marpolbul.2012.05.008, 2012.



861 Espinoza Villar, R., Martinez, J. M., Le Texier, M., Guyot, J. L., Fraizy, P., Meneses, P. R. and Oliveira,  
862 E. de: A study of sediment transport in the Madeira River, Brazil, using MODIS remote-sensing  
863 images, *J. South Am. Earth Sci.*, 44, 45–54, doi:10.1016/j.jsames.2012.11.006, 2013.

864 Fabricius, K. E.: Effects of terrestrial runoff on the ecology of corals and coral reefs: Review and  
865 synthesis, *Mar. Pollut. Bull.*, 50(2), 125–146, doi:10.1016/j.marpolbul.2004.11.028, 2005.

866 Fabricius, K. E., Logan, M., Weeks, S. J., Lewis, S. E. and Brodie, J.: Changes in water clarity in  
867 response to river discharges on the Great Barrier Reef continental shelf: 2002–2013, *Estuar. Coast.  
868 Shelf Sci.*, 173, A1–A15, doi:10.1016/j.ecss.2016.03.001, 2016.

869 Gaveau, D. L. A., Sheil, D., Salim, M. A., Arjasakusuma, S., Ancrenaz, M., Pacheco, P. and Meijaard, E.:  
870 Rapid conversions and avoided deforestation : examining four decades of industrial plantation  
871 expansion in Borneo, *Nat. Publ. Gr.*, (September), 1–13, doi:10.1038/srep32017, 2016.

872 Gilmour, J. P., Cooper, T. F., Fabricius, K. E. and Smith, L. D.: Early warning indicators of change in the  
873 condition of corals and coral communities in response to key anthropogenic stressors in the Pilbara,  
874 Western Australia, *Aust. Inst. Mar. Sci. Rep. to Environ. Prot. Authority*. 101pp, 2006.

875 Giuliani, G., Chatenoux, B., Piller, T., Moser, F. and Lacroix, P.: Data Cube on Demand (DCoD):  
876 Generating an earth observation Data Cube anywhere in the world, *Int. J. Appl. Earth Obs. Geoinf.*,  
877 87(December 2019), 102035, doi:10.1016/j.jag.2019.102035, 2020.

878 Gomes, V. C. F., Carlos, F. M., Queiroz, G. R., Ferreira, K. R. and Santos, R.: Accessing and Processing  
879 Brazilian Earth Observation Data Cubes With the Open Data Cube Platform, *ISPRS Ann. Photogramm.  
880 Remote Sens. Spat. Inf. Sci.*, V-4–2021, 153–159, doi:10.5194/isprs-annals-v-4-2021-153-2021, 2021.

881 Gomyo, M. and Koichiro, K.: Spatial and temporal variations in rainfall and the ENSO-rainfall  
882 relationship over Sarawak, Malaysian Borneo, *Sci. Online Lett. Atmos.*, 5, 41–44,  
883 doi:10.2151/sola.2009-011, 2009.

884 González Vilas, L., Spyrakos, E. and Torres Palenzuela, J. M.: Neural network estimation of  
885 chlorophyll-a from MERIS full resolution data for the coastal waters of Galician rias (NW Spain),  
886 *Remote Sens. Environ.*, 115(2), 524–535, doi:10.1016/j.rse.2010.09.021, 2011.

887 Ha, N. T. T., Thao, N. T. P., Koike, K. and Nhuan, M. T.: Selecting the best band ratio to estimate  
888 chlorophyll-a concentration in a tropical freshwater lake using sentinel 2A images from a case study  
889 of Lake Ba Be (Northern Vietnam), *ISPRS Int. J. Geo-Information*, 6(9), doi:10.3390/ijgi6090290,  
890 2017.

891 Henley, W. F., Patterson, M. A., Neves, R. J. and Dennis Lemly, A.: Effects of Sedimentation and  
892 Turbidity on Lotic Food Webs: A Concise Review for Natural Resource Managers, *Rev. Fish. Sci.*, 8(2),  
893 125–139, doi:10.1080/10641260091129198, 2000.

894 Hodgson, G.: Tetracycline reduces sedimentation damage to corals, *Mar. Biol.*, 104(3), 493–496,  
895 1990.

896 Hon, J. and Shibata, S.: A Review on Land Use in the Malaysian State of Sarawak, Borneo and  
897 Recommendations for Wildlife Conservation Inside Production Forest Environment, *Borneo J.  
898 Resour. Sci. Technol.*, 3(2), 22–35, doi:10.33736/bjrst.244.2013, 2013.

899 Horsburgh, J. S., Spackman, A., Stevens, D. K., Tarboton, D. G. and Mesner, N. O.: Environmental  
900 Modelling & Software A sensor network for high frequency estimation of water quality constituent  
901 fluxes using surrogates, , 25, 1031–1044, doi:10.1016/j.envsoft.2009.10.012, 2010.

902 Howarth, R. W.: Coastal nitrogen pollution: A review of sources and trends globally and regionally,  
903 *Harmful Algae*, 8(1), 14–20, doi:10.1016/j.hal.2008.08.015, 2008.

904 Hu, C., Lee, Z. and Franz, B.: Chlorophyll a algorithms for oligotrophic oceans: A novel approach  
905 based on three-band reflectance difference, *J. Geophys. Res. Ocean.*, 117(1), 1–25,  
906 doi:10.1029/2011JC007395, 2012.

907 Jiang, D., Matsushita, B., Pahlevan, N., Gurlin, D., Lehmann, M. K., Fichot, C. G., Schalles, J., Loisel, H.,  
908 Binding, C., Zhang, Y., Alikas, K., Kangro, K., Uusõue, M., Ondrusek, M., Greb, S., Moses, W. J.,  
909 Lohrenz, S. and O'Donnell, D.: Remotely estimating total suspended solids concentration in clear to  
910 extremely turbid waters using a novel semi-analytical method, *Remote Sens. Environ.*, 258,  
911 doi:10.1016/j.rse.2021.112386, 2021.

912 Jiang, H. and Liu, Y.: Monitoring of TSS concentration in Poyang Lake based on MODIS data, *Yangtze  
913 River*, 42(17), 87–90, 2011.

914 Kemp, P., Sear, D., Collins, A., Naden, P. and Jones, I.: The impacts of fine sediment on riverine fish,  
915 *Hydrol. Process.*, 25(11), 1800–1821, doi:10.1002/hyp.7940, 2011.

916 Killough, B.: The Impact of Analysis Ready Data in the Africa Regional Data Cube, *Int. Geosci. Remote  
917 Sens. Symp.*, (July 2019), 5646–5649, doi:10.1109/IGARSS.2019.8898321, 2019.

918 Kim, H. C., Son, S., Kim, Y. H., Khim, J. S., Nam, J., Chang, W. K., Lee, J. H., Lee, C. H. and Ryu, J.:  
919 Remote sensing and water quality indicators in the Korean West coast: Spatio-temporal structures of  
920 MODIS-derived chlorophyll-a and total suspended solids, *Mar. Pollut. Bull.*, 121(1–2), 425–434,  
921 doi:10.1016/j.marpolbul.2017.05.026, 2017.

922 Krause, C., Dunn, B., Bishop-Taylor, R., Adams, C., Burton, C., Alger, M., Chua, S., Phillips, C., Newey,  
923 V., Kouzoubov, K., Leith, A., Ayers, D., Hicks, A. and DEA Notebooks contributors 2021: Digital Earth  
924 Australia notebooks and tools repository, , doi:https://doi.org/10.26186/145234, 2021.

925 Kuok, K. K., Chiu, P., Yap, A. and Law, K.: Determination of the Best Tank Model for the Southern  
926 Region of Sarawak Determination Number of Tanks for Tank Model at Southern Region of Sarawak, ,  
927 (August 2012), 2018.

928 Langer, O. E.: Effects of sedimentation on salmonid stream life, *Environmental Protection Service.*,  
929 1980.

930 Lavigne, H., Van der Zande, D., Ruddick, K., Cardoso Dos Santos, J. F., Gohin, F., Brotas, V. and  
931 Kratzer, S.: Quality-control tests for OC4, OC5 and NIR-red satellite chlorophyll-a algorithms applied  
932 to coastal waters, *Remote Sens. Environ.*, 255, 112237, doi:10.1016/j.rse.2020.112237, 2021.

933 Lee, K. H., Noh, J. and Khim, J. S.: The Blue Economy and the United Nations' sustainable  
934 development goals: Challenges and opportunities, *Environ. Int.*, 137(October 2019), 105528,  
935 doi:10.1016/j.envint.2020.105528, 2020a.

936 Lee, W. C., Viswanathan, K. K., Kamri, T. and King, S.: Status of Sarawak Fisheries: Challenges and  
937 Way Forward, *Int. J. Serv. Manag. Sustain.*, 5(2), 187–200, doi:10.24191/ijms.v5i2.11719, 2020b.

938 Lehner, B., Verdin, K. and Jarvis, A.: HydroSHEDS technical documentation, *World Wildl. Fund US*,  
939 Washington, DC, 1–27, 2006.

940 Lemley, D. A., Adams, J. B., Bornman, T. G., Campbell, E. E. and Deyzel, S. H. P.: Land-derived  
941 inorganic nutrient loading to coastal waters and potential implications for nearshore plankton  
942 dynamics, *Cont. Shelf Res.*, 174(August 2018), 1–11, doi:10.1016/j.csr.2019.01.003, 2019.

943 Lewis, A., Oliver, S., Lymburner, L., Evans, B., Wyborn, L., Mueller, N., Raevksi, G., Hooke, J.,  
944 Woodcock, R., Sixsmith, J., Wu, W., Tan, P., Li, F., Killough, B., Minchin, S., Roberts, D., Ayers, D.,  
945 Bala, B., Dwyer, J., Dekker, A., Dhu, T., Hicks, A., Ip, A., Purss, M., Richards, C., Sagar, S., Trenham, C.,  
946 Wang, P. and Wang, L. W.: The Australian Geoscience Data Cube — Foundations and lessons

947 learned, *Remote Sens. Environ.*, 202, 276–292, doi:10.1016/j.rse.2017.03.015, 2017.

948 Limcih, F., Jilnm, M., Hb, H., Ilcach, H. N. M., Mnl, F., Fi, F. and Nb, F.: Study of Coastal Areas in Miri,  
949 in *World Engineering Congress 2010*, pp. 56–65., 2010.

950 Ling, T. Y., Soo, C. L., Sivalingam, J. R., Nyanti, L., Sim, S. F. and Grinang, J.: Assessment of the Water  
951 and Sediment Quality of Tropical Forest Streams in Upper Reaches of the Baleh River, Sarawak,  
952 Malaysia, Subjected to Logging Activities, *J. Chem.*, 2016, doi:10.1155/2016/8503931, 2016.

953 Liu, B., D'Sa, E. J. and Joshi, I.: Multi-decadal trends and influences on dissolved organic carbon  
954 distribution in the Barataria Basin, Louisiana from in-situ and Landsat/MODIS observations, *Remote  
955 Sens. Environ.*, 228(May), 183–202, doi:10.1016/j.rse.2019.04.023, 2019.

956 Loisel, H., Mangin, A., Vantrepotte, V., Dessailly, D., Ngoc Dinh, D., Garnesson, P., Ouillon, S.,  
957 Lefebvre, J. P., Mériaux, X. and Minh Phan, T.: Variability of suspended particulate matter  
958 concentration in coastal waters under the Mekong's influence from ocean color (MERIS) remote  
959 sensing over the last decade, *Remote Sens. Environ.*, 150, 218–230, doi:10.1016/j.rse.2014.05.006,  
960 2014.

961 Long, S. M.: Sarawak Coastal Biodiversity : A Current Status, *Kuroshio Sci.*, 8(1), 71–84 [online]  
962 Available from: <https://www.researchgate.net/publication/265793245>, 2014.

963 Lu, Y., Yuan, J., Lu, X., Su, C., Zhang, Y., Wang, C., Cao, X., Li, Q., Su, J., Ittekkot, V., Garbutt, R. A.,  
964 Bush, S., Fletcher, S., Wagey, T., Kachur, A. and Sweijd, N.: Major threats of pollution and climate  
965 change to global coastal ecosystems and enhanced management for sustainability, *Environ. Pollut.*,  
966 239, 670–680, doi:10.1016/j.envpol.2018.04.016, 2018.

967 Macklin, M. G., Jones, A. F. and Lewin, J.: River response to rapid Holocene environmental change:  
968 evidence and explanation in British catchments, *Quat. Sci. Rev.*, 29(13–14), 1555–1576,  
969 doi:10.1016/j.quascirev.2009.06.010, 2010.

970 Mao, Z., Chen, J., Pan, D., Tao, B. and Zhu, Q.: A regional remote sensing algorithm for total  
971 suspended matter in the East China Sea, *Remote Sens. Environ.*, 124, 819–831,  
972 doi:10.1016/j.rse.2012.06.014, 2012.

973 Martin, P., Cherukuru, N., Tan, A. S. Y., Sanwlani, N., Mujahid, A. and Müller, M.: Distribution and  
974 cycling of terrigenous dissolved organic carbon in peatland-draining rivers and coastal waters of  
975 Sarawak, Borneo, *Biogeosciences*, 15(22), 6847–6865, doi:10.5194/bg-15-6847-2018, 2018.

976 Mengen, D., Ottinger, M., Leinenkugel, P. and Ribbe, L.: Modeling river discharge using automated  
977 river width measurements derived from sentinel-1 time series, *Remote Sens.*, 12(19), 1–24,  
978 doi:10.3390/rs12193236, 2020.

979 Milliman, J. D. and Farnsworth, K. L.: *River discharge to the coastal ocean: a global synthesis*,  
980 Cambridge University Press., 2013.

981 Mohammad Razi, M. A., Mokhtar, A., Mahamud, M., Rahmat, S. N. and Al-Gheethi, A.: Monitoring of  
982 river and marine water quality at Sarawak baseline, *Environ. Forensics*, 22(1–2), 219–240,  
983 doi:10.1080/15275922.2020.1836076, 2021.

984 Morel, A. and Bélanger, S.: Improved detection of turbid waters from ocean color sensors  
985 information, *Remote Sens. Environ.*, 102(3–4), 237–249, doi:10.1016/j.rse.2006.01.022, 2006.

986 Morel, A. and Gentili, B.: A simple band ratio technique to quantify the colored dissolved and detrital  
987 organic material from ocean color remotely sensed data, *Remote Sens. Environ.*, 113(5), 998–1011,  
988 doi:10.1016/j.rse.2009.01.008, 2009.

989 Mueller, J., Mueller, J., Pietras, C., Hooker, S., Clark, D., Frouin, A., Mitchell, B., Bidigare, R., Trees, C.

990 and Werdell, J.: Ocean Optics Protocols For Satellite Ocean Color Sensor Validation, Revision 3,  
991 volumes 1 and 2., 2002.

992 Müller-dum, D., Warneke, T., Rixen, T., Müller, M., Baum, A., Christodoulou, A., Oakes, J., Eyre, B. D.  
993 and Notholt, J.: Impact of peatlands on carbon dioxide ( CO<sub>2</sub> ) emissions from the Rajang River and  
994 Estuary , Malaysia, , 17–32, 2019.

995 Müller, D., Warneke, T., Rixen, T., Müller, M., Mujahid, A., Bange, H. W. and Notholt, J.: Fate of  
996 terrestrial organic carbon and associated CO<sub>2</sub> and CO emissions from two Southeast Asian estuaries,  
997 Biogeosciences, 13(3), 691–705, doi:10.5194/bg-13-691-2016, 2016.

998 NASA Official: Ocean Level-2 Data Format Specification, [online] Available from:  
999 <https://oceancolor.gsfc.nasa.gov/docs/format/l2nc/>, n.d.

1000 Nazirova, K., Alferyeva, Y., Lavrova, O., Shur, Y., Soloviev, D., Bocharova, T. and Stochkov, A.:  
1001 Comparison of in situ and remote-sensing methods to determine turbidity and concentration of  
1002 suspended matter in the estuary zone of the mzymta river, black sea, Remote Sens., 13(1), 1–29,  
1003 doi:10.3390/rs13010143, 2021.

1004 Neil, C., Spyarakos, E., Hunter, P. D. and Tyler, A. N.: A global approach for chlorophyll-a retrieval  
1005 across optically complex inland waters based on optical water types, Remote Sens. Environ.,  
1006 229(May), 159–178, doi:10.1016/j.rse.2019.04.027, 2019.

1007 Ondrusek, M., Stengel, E., Kinkade, C. S., Vogel, R. L., Keegstra, P., Hunter, C. and Kim, C.: The  
1008 development of a new optical total suspended matter algorithm for the Chesapeake Bay, Remote  
1009 Sens. Environ., 119, 243–254, doi:10.1016/j.rse.2011.12.018, 2012.

1010 Open Data Cube: Open Data Cube, [online] Available from:  
1011 <https://opendatacube.readthedocs.io/en/latest/user/intro.html> (Accessed 25 October 2021), 2021.

1012 Park, G. S.: The role and distribution of total suspended solids in the macrotidal coastal waters of  
1013 Korea, Environ. Monit. Assess., 135(1–3), 153–162, doi:10.1007/s10661-007-9640-3, 2007.

1014 Petus, C., Marieu, V., Novoa, S., Chust, G., Bruneau, N. and Froidefond, J. M.: Monitoring spatio-  
1015 temporal variability of the Adour River turbid plume (Bay of Biscay, France) with MODIS 250-m  
1016 imagery, Cont. Shelf Res., 74, 35–49, doi:10.1016/j.csr.2013.11.011, 2014.

1017 Praveena, S. M., Siraj, S. S. and Aris, A. Z.: Coral reefs studies and threats in Malaysia: A mini review,  
1018 Rev. Environ. Sci. Biotechnol., 11(1), 27–39, doi:10.1007/s11157-011-9261-8, 2012.

1019 Ramaswamy, V., Rao, P. S., Rao, K. H., Thwin, S., Rao, N. S. and Raiker, V.: Tidal influence on  
1020 suspended sediment distribution and dispersal in the northern Andaman Sea and Gulf of Martaban,  
1021 Mar. Geol., 208(1), 33–42, doi:10.1016/j.margeo.2004.04.019, 2004.

1022 Refaeilzadeh, P., Tang, L., Liu, H., Angeles, L. and Scientist, C. D.: Encyclopedia of Database Systems,  
1023 Encycl. Database Syst., doi:10.1007/978-1-4899-7993-3, 2020.

1024 Risk, M. J. and Edinger, E.: Impacts of sediment on coral reefs, Encycl. Mod. coral reefs. Springer,  
1025 Netherlands, 575–586, 2011.

1026 Rogers, C. S.: The effect of shading on coral reef structure and function, J. Exp. Mar. Bio. Ecol., 41(3),  
1027 269–288, doi:10.1016/0022-0981(79)90136-9, 1979.

1028 Sa’adi, Z., Shahid, S., Chung, E. S. and Ismail, T. bin: Projection of spatial and temporal changes of  
1029 rainfall in Sarawak of Borneo Island using statistical downscaling of CMIP5 models, Atmos. Res.,  
1030 197(November 2016), 446–460, doi:10.1016/j.atmosres.2017.08.002, 2017.

1031 Sandifer, P. A., Keener, P., Scott, G. I. and Porter, D. E.: Oceans and Human Health and the New Blue

- 1032 Economy, Elsevier Inc., 2021.
- 1033 Sarawak Forestry Corporation: Maludam National Park, [online] Available from:  
1034 <https://sarawakforestry.com/parks-and-reserves/maludam-national-park/>, 2022.
- 1035 Seegers, B. N., Stumpf, R. P., Schaeffer, B. A., Loftin, K. A. and Werdell, P. J.: Performance metrics for  
1036 the assessment of satellite data products: an ocean color case study, *Opt. Express*, 26(6), 7404,  
1037 doi:10.1364/oe.26.007404, 2018.
- 1038 Shaw, E. Al and Richardson, J. S.: Direct and indirect effects of sediment pulse duration on stream  
1039 invertebrate assemblages and rainbow trout (*Oncorhynchus mykiss*) growth and survival, *Can. J.*  
1040 *Fish. Aquat. Sci.*, 58(11), 2213–2221, doi:10.1139/f01-160, 2001.
- 1041 Sim, C., Cherukuru, N., Mujahid, A., Martin, P., Sanwlani, N., Warneke, T., Rixen, T., Notholt, J. and  
1042 Müller, M.: A new remote sensing method to estimate river to ocean DOC flux in peatland  
1043 dominated Sarawak coastal regions, Borneo, *Remote Sens.*, 12(20), 1–13, doi:10.3390/rs12203380,  
1044 2020.
- 1045 Siswanto, E., Tang, J. and Yamaguchi, H.: Empirical ocean-color algorithms to retrieve chlorophyll- a ,  
1046 total suspended matter , and colored dissolved organic matter absorption coefficient in the Yellow  
1047 and East China Seas , 627–650, doi:10.1007/s10872-011-0062-z, 2011.
- 1048 Slonecker, E. T., Jones, D. K. and Pellerin, B. A.: The new Landsat 8 potential for remote sensing of  
1049 colored dissolved organic matter (CDOM), *Mar. Pollut. Bull.*, 107(2), 518–527,  
1050 doi:10.1016/j.marpolbul.2016.02.076, 2016.
- 1051 Song, C., Wang, G., Sun, X., Chang, R. and Mao, T.: Control factors and scale analysis of annual river  
1052 water, sediments and carbon transport in China, *Sci. Rep.*, 6(May), 1–14, doi:10.1038/srep25963,  
1053 2016.
- 1054 Song, Z., Shi, W., Zhang, J., Hu, H., Zhang, F. and Xu, X.: Transport mechanism of suspended  
1055 sediments and migration trends of sediments in the central hangzhou bay, *Water (Switzerland)*,  
1056 12(8), doi:10.3390/W12082189, 2020.
- 1057 Soo, C. L., Chen, C. A. and Mohd-Long, S.: Assessment of Near-Bottom Water Quality of  
1058 Southwestern Coast of Sarawak, Borneo, Malaysia: A Multivariate Statistical Approach, *J. Chem.*,  
1059 2017, doi:10.1155/2017/1590329, 2017.
- 1060 Soum, S., Ngor, P. B., Dilts, T. E., Lohani, S., Kelson, S., Null, S. E., Tromboni, F., Hogan, Z. S., Chan, B.  
1061 and Chandra, S.: Spatial and long-term temporal changes in water quality dynamics of the tonle sap  
1062 ecosystem, *Water (Switzerland)*, 13(15), doi:10.3390/w13152059, 2021.
- 1063 Staub, J. R. and Esterle, J. S.: Provenance and sediment dispersal in the Rajang River delta/coastal  
1064 plain system, Sarawak, East Malaysia, *Sediment. Geol.*, 85(1–4), 191–201, doi:10.1016/0037-  
1065 0738(93)90083-H, 1993.
- 1066 Staub, J. R., Among, H. L. and Gastaldo, R. A.: Seasonal sediment transport and deposition in the  
1067 Rajang River delta, Sarawak, East Malaysia, *Sediment. Geol.*, 133(3–4), 249–264, doi:10.1016/S0037-  
1068 0738(00)00042-7, 2000.
- 1069 Sun, C.: Riverine influence on ocean color in the equatorial South China Sea, *Cont. Shelf Res.*,  
1070 143(December 2015), 151–158, doi:10.1016/j.csr.2016.10.008, 2017a.
- 1071 Sun, C.: Riverine influence on ocean color in the equatorial South China Sea, *Cont. Shelf Res.*,  
1072 143(October 2016), 151–158, doi:10.1016/j.csr.2016.10.008, 2017b.
- 1073 Sutherland, A. B. and Meyer, J. L.: Effects of increased suspended sediment on growth rate and gill  
1074 condition of two southern Appalachian minnows, *Environ. Biol. Fishes*, 80(4), 389–403,

1075 doi:10.1007/s10641-006-9139-8, 2007.

1076 Swain, R. and Sahoo, B.: Mapping of heavy metal pollution in river water at daily time-scale using  
1077 spatio-temporal fusion of MODIS-aqua and Landsat satellite imageries, *J. Environ. Manage.*, 192, 1–  
1078 14, doi:10.1016/j.jenvman.2017.01.034, 2017.

1079 Tangang, F. T., Juneng, L., Salimun, E., Sei, K. M., Le, L. J. and Muhamad, H.: Climate change and  
1080 variability over Malaysia: Gaps in science and research information, *Sains Malaysiana*, 41(11), 1355–  
1081 1366, 2012.

1082 Tawan, A. S., Ling, T. Y., Nyanti, L., Sim, S. F., Grinang, J., Soo, C. L., Lee, K. S. P. and Ganyai, T.:  
1083 Assessment of water quality and pollutant loading of the Rajang River and its tributaries at Pelagus  
1084 area subjected to seasonal variation and river regulation, *Environ. Dev. Sustain.*, 22(5), 4101–4124,  
1085 doi:10.1007/s10668-019-00374-9, 2020.

1086 Telesnicki, G. J. and Goldberg, W. M.: CORAL REEF PAPER EFFECTS OF TURBIDITY ON THE  
1087 PHOTOSYNTHESIS AND RESPIRATION OF TWO SOUTH FLORIDA REEF CORAL SPECIES portant factors  
1088 in the regulation of coral cover , diversity , and abundance ( Ed- ships between suspended sediment  
1089 concentrations or parti , , 57(2), 527–539, 1995.

1090 Tilburg, C. E., Jordan, L. M., Carlson, A. E., Zeeman, S. I. and Yund, P. O.: The effects of precipitation,  
1091 river discharge, land use and coastal circulation on water quality in coastal Maine, *R. Soc. Open Sci.*,  
1092 2(7), doi:10.1098/rsos.140429, 2015.

1093 Tromboni, F., Dilts, T. E., Null, S. E., Lohani, S., Ngor, P. B., Soum, S., Hogan, Z. and Chandra, S.:  
1094 Changing land use and population density are degrading water quality in the lower mekong basin,  
1095 *Water (Switzerland)*, 13(14), 1–16, doi:10.3390/w13141948, 2021.

1096 United Nations: The Ocean Conference, in *The Ocean Conference*, vol. 53, p. 130, New York., 2017.

1097 Valerio, A. de M., Kampel, M., Vantrepotte, V., Ward, N. D., Sawakuchi, H. O., Less, D. F. D. S., Neu,  
1098 V., Cunha, A. and Richey, J.: Using CDOM optical properties for estimating DOC concentrations and  
1099 pCO<sub>2</sub> in the Lower Amazon River , *Opt. Express*, 26(14), A657, doi:10.1364/oe.26.00a657, 2018.

1100 Verschelling, E., van der Deijl, E., van der Perk, M., Sloff, K. and Middelkoop, H.: Effects of discharge,  
1101 wind, and tide on sedimentation in a recently restored tidal freshwater wetland, *Hydrol. Process.*,  
1102 31(16), 2827–2841, doi:10.1002/hyp.11217, 2017.

1103 Vijith, H., Hurmain, A. and Dodge-Wan, D.: Impacts of land use changes and land cover alteration on  
1104 soil erosion rates and vulnerability of tropical mountain ranges in Borneo, *Remote Sens. Appl. Soc.*  
1105 *Environ.*, 12(September), 57–69, doi:10.1016/j.rsase.2018.09.003, 2018.

1106 Wang, C., Chen, S., Li, D., Wang, D., Liu, W. and Yang, J.: A Landsat-based model for retrieving total  
1107 suspended solids concentration of estuaries and coasts in China, *Geosci. Model Dev.*, 10(12), 4347–  
1108 4365, doi:10.5194/gmd-10-4347-2017, 2017.

1109 Wang, J., Tong, Y., Feng, L., Zhao, D., Zheng, C. and Tang, J.: Satellite-Observed Decreases in Water  
1110 Turbidity in the Pearl River Estuary: Potential Linkage With Sea-Level Rise, *J. Geophys. Res. Ocean.*,  
1111 126(4), 1–17, doi:10.1029/2020JC016842, 2021.

1112 Weber, M., Lott, C. and Fabricius, K. E.: Sedimentation stress in a scleractinian coral exposed to  
1113 terrestrial and marine sediments with contrasting physical, organic and geochemical properties, *J.*  
1114 *Exp. Mar. Bio. Ecol.*, 336(1), 18–32, doi:10.1016/j.jembe.2006.04.007, 2006.

1115 Werdell, P. J., McKinna, L. I. W., Boss, E., Ackleson, S. G., Craig, S. E., Gregg, W. W., Lee, Z.,  
1116 Maritorena, S., Roesler, C. S., Rousseaux, C. S., Stramski, D., Sullivan, J. M., Twardowski, M. S.,  
1117 Tzortziou, M. and Zhang, X.: An overview of approaches and challenges for retrieving marine

1118 inherent optical properties from ocean color remote sensing, *Prog. Oceanogr.*, 160, 186–212,  
1119 doi:10.1016/j.pocean.2018.01.001, 2018.

1120 Whitmore, T. C.: Tropical rain forests of the Par East, Oxford. Clarendon Press., 1984.

1121 Wilber, D. H. and Clarke, D. G.: Biological Effects of Suspended Sediments: A Review of Suspended  
1122 Sediment Impacts on Fish and Shellfish with Relation to Dredging Activities in Estuaries, *North Am. J.*  
1123 *Fish. Manag.*, 21(4), 855–875, doi:10.1577/1548-8675(2001)021<0855:beossa>2.0.co;2, 2001.

1124 World Bank and United Nations Department of Economic and Social Affairs (UNDESA): The Potential  
1125 of the Blue Economy: Increasing Long-term Benefits of the Sustainable Use of Marine Resources for  
1126 Small Island Developing States and Coastal Least Developed Countries, World Bank, Washington DC.,  
1127 2017.

1128 Wu, C. S., Yang, S. L. and Lei, Y. ping: Quantifying the anthropogenic and climatic impacts on water  
1129 discharge and sediment load in the Pearl River (Zhujiang), China (1954-2009), *J. Hydrol.*, 452–453,  
1130 190–204, doi:10.1016/j.jhydrol.2012.05.064, 2012.

1131 Yang, S. L., Zhao, Q. Y. and Belkin, I. M.: Temporal variation in the sediment load of the Yangtze river  
1132 and the influences of human activities, *J. Hydrol.*, 263(1–4), 56–71, doi:10.1016/S0022-  
1133 1694(02)00028-8, 2002.

1134 Zhan, W., Wu, J., Wei, X., Tang, S. and Zhan, H.: Spatio-temporal variation of the suspended  
1135 sediment concentration in the Pearl River Estuary observed by MODIS during 2003–2015, *Cont. Shelf*  
1136 *Res.*, 172(May 2018), 22–32, doi:10.1016/j.csr.2018.11.007, 2019.

1137 Zhang, L. J., Wang, L., Cai, W. J., Liu, D. M. and Yu, Z. G.: Impact of human activities on organic carbon  
1138 transport in the Yellow River, *Biogeosciences*, 10(4), 2513–2524, doi:10.5194/bg-10-2513-2013,  
1139 2013.

1140 Zhang, M., Tang, J., Dong, Q., Song, Q. T. and Ding, J.: Retrieval of total suspended matter  
1141 concentration in the Yellow and East China Seas from MODIS imagery, *Remote Sens. Environ.*,  
1142 114(2), 392–403, doi:10.1016/j.rse.2009.09.016, 2010a.

1143 Zhang, Y., Lin, S., Liu, J., Qian, X. and Ge, Y.: Time-series MODIS image-based retrieval and  
1144 distribution analysis of total suspended matter concentrations in Lake Taihu (China), *Int. J. Environ.*  
1145 *Res. Public Health*, 7(9), 3545–3560, doi:10.3390/ijerph7093545, 2010b.

1146 Zhou, Y., Xuan, J. and Huang, D.: Tidal variation of total suspended solids over the Yangtze Bank  
1147 based on the geostationary ocean color imager, *Sci. China Earth Sci.*, 63(9), 1381–1389,  
1148 doi:10.1007/s11430-019-9618-7, 2020.

1149

1150

1151

1152

1153

1154

1155

1156

1157

1158

1159

1160

1161

1162

1163

1164

1165